Ecological facilitation may hinder adaptation to climate change in a stressful environment

Raphaël Scherrer[1,*], Megan Korte[1,2], G. Sander van Doorn[1], and Rampal S. Etienne[1]

[1]Groningen Institute for Evolutionary Life Sciences, University of Groningen, Groningen, the Netherlands

[2]Center for Conservation Biology, University of California, Riverside, California, USA

[*]Corresponding author: raphael.scherrer@evobio.eu

Abstract

Many plants, in (semi-)arid ecosystems in particular, rely on so-called nurse plants for protection and growth, in a species interaction called ecological facilitation. However, it is not clear whether facilitation will protect the facilitated plant from extinction if the environmental conditions change, for example due to climate change. Here, we use an evolutionary model to study the impact of ecological facilitation on the adaptive potential of an annual plant facilitated by nurse shrubs under a changing climate, specifically, when the landscape becomes more arid. We find that two alternative strategies can arise: a stress-tolerant strategy, capable of surviving outside the facilitated patches as well as underneath shrubs, but at a fecundity cost; and a stress-sensitive strategy, with a higher reproductive output but confined to the facilitated patches. Under some conditions, these two strategies can coexist. The presence of the stress-tolerant strategy is key to preventing extinction when the climate causes more stress (drought). By running three different climate change scenarios (stress increase under the shrubs, whole-landscape deterioration and shrub-cover shrinkage), we find that a trade-off between fecundity and stress tolerance usually traps an initially stress-sensitive population into staying sensitive even as the facilitated patches recede under climate change. The population then continues to rely on facilitation, and is unable to evolve stress tolerance before it is too late and extinction is unavoidable. By contrast, an increase in stress in the facilitated areas, with or without an increase in stress outside of the facilitated areas, readily promotes adaptation to increasingly severe aridity. Thus, persistence of sheltered areas in a patchy landscape may prevent adaptation to the harsher surroundings, putting the population at risk of extinction in a changing climate.

Keywords — stress tolerance, evolutionary rescue, extinction, habitat heterogeneity, adaptive dynamics, metapopulation

1

Introduction

Global climate change is threatening to increase the degradation of ecosystems worldwide, and has far-reaching consequences on populations of organisms, particularly in plant communities (Franklin et al., 2016). Ecosystems that already endure stressful environmental conditions are especially susceptible to adverse manifestations of climate change, such as amplification of heat waves and water shortages in arid and semi-arid regions, which are at high risk of desertification over the next decades (D'Odorico et al., 2013; Vicente-Serrano et al., 2014). It is thus crucial to examine the mechanisms promoting community resilience that could alleviate stressors on plant communities to prevent further decline.

Interspecific facilitation is a widespread type of ecological interaction in many of the world's ecosystems, and one particularly known to play a key role in plant community structure. In interspecific facilitation, a nurse or benefactor species (which is adapted to local environmentally stressful conditions) positively affects a spatially associated beneficiary species (which is then better able to survive and/or reproduce in this environment; Bruno et al., 2003). This allows many species to cope with stressful climates where their potential to thrive would otherwise be seriously impacted (Bertness & Callaway, 1994; Callaway, 2007a, 2007b). For example, the observation that in some plant communities 90% of the species are found only beneath the canopies of perennial plants has led authors to propose facilitation as a key force maintaining biodiversity in those ecosystems (Valiente-Banuet & Verdú, 2007).

Facilitated patches of vegetation provide buffered microclimates for many populations that struggle to survive environmental stressors and as such, contribute to environmental heterogeneity in harsh habitats (Armas et al., 2008; Pugnaire et al., 2011; Hannah et al., 2014; Suggitt et al., 2018). This, in turn, can have profound consequences for evolutionary processes and local adaptation in the beneficiary species (O'Brien et al., 2020), sometimes at the microgeographic scale (Richardson et al., 2014; O'Brien et al., 2020; Verdú et al., 2021). Typical facilitated microhabitats are characterized by milder and/or more enriched conditions with respect to temperature, humidity or nutrients, in contrast to the open landscape (Armas & Pugnaire, 2005; Wright et al., 2005; Prieto et al., 2010). They may also be the theater of more intense competition (Adler et al., 2018), but that is not necessarily always the case (Raath-Krüger et al., 2021). By affecting habitat heterogeneity in this way, facilitation in harsh landscapes may have profound consequences on the eco-evolutionary dynamics of beneficiary species, especially in the face of a changing climate. How exactly the environmental heterogeneity brought about by ecological facilitation affects the adaptive potential of the beneficiary populations is less well understood, however, and the idea that facilitation always positively affects adaptation in the beneficiary species has been subject to debate.

The idea that facilitation may foster adaptation comes from several lines of evidence. First, facilitation can expand the geographical range over which a species can occur and therefore can give it a head start, in the form of a higher global population size, in the race to avoid extinction (Bruno et al., 2003; Armas et al., 2011; Soliveres et al., 2011). This was proposed

for the alga *Mazzaella laminarioides*, whose establishment probability is increased in harsher environments at the edge of its range, thanks to benefactor barnacles (Aguilera et al., 2015). Alternatively, as a form of niche construction, facilitation may play a similar role to phenotypic plasticity in exposing organisms to environments they would otherwise not experience, setting up the stage for genetic assimilation and adaptation (Day et al., 2003; Flatt, 2005; Chevin & Lande, 2011; Laland et al., 2016; Chevin & Hoffmann, 2017). Relaxed selection in sheltered environments may also contribute to the accumulation of cryptic genetic variation, which may become adaptive in the context of a changing environment (Gibson & Dworkin, 2004; Badyaev, 2005; Ledón-Rettig et al., 2014; Paaby & Rockman, 2014). Finally, facilitation may promote survival in the face of a changing climate in the absence of adaptation, by allowing beneficiary species to keep their ancestral niche through associations with benefactor species. This has been suggested as an explanation for the observation that many mesophilic Tertiary plant lineages that survived the transition to the drier Quaternary climate are now found in facilitative associations with benefactor xerophilic species in semi-arid and Mediterranean ecosystems (Valiente-Banuet et al., 2006; Valiente-Banuet & Verdú, 2007; Hampe & Jump, 2011).

In contrast, facilitation may also hamper adaptation. Gene flow among populations adapted to different microhabitats in a heterogeneous landscape is known to curb local adaptation, offering one powerful explanation for why species are restricted in space (e.g. García-Ramos and Kirkpatrick, 1997; Kirkpatrick and Barton, 1997; Lenormand, 2002). Facilitation could play a similar inhibitory role in the emergence of ecotypes adapted to new, harsher environments (Liancourt et al., 2012), not only because of maladaptive gene flow but also hybrid rescue (which would prevent the full divergence and speciation of a new ecotype by providing shelter to otherwise maladapted hybrids). Furthermore, adaptation to harsh habitats is restricted by the amount of genetic variation for adaptive traits (Lande & Shannon, 1996; Barton, 2001; Tufto, 2001; Gilbert & Whitlock, 2017), and new adaptive alleles are unlikely to arise in marginal habitats with low population densities (Orr & Unckless, 2008). Moreover, harsh environments close to the limits of the fundamental niche of a species (demographic 'sinks') are thought to be notoriously difficult to adapt to, because the strength of selection is lower where fitness (and density) is lower (Brown & Pavlovic, 1992; Holt & Gaines, 1992; Kawecki, 1995; Kawecki & Holt, 2002; Holt et al., 2003).

A resolution of the debate about the role of facilitation in adaptation may be aided by turning to the general theoretical literature on local adaptation in heterogeneous landscapes (Holt, 2003; Kawecki, 2004; Holt et al., 2005; Bridle & Vines, 2007; Kawecki, 2008; Holt & Barfield, 2011; Angert et al., 2020). This literature is vast and has shown that adaptation is complicated by many factors, such as stochastic effects in small demes (Glémin et al., 2003; Alleaume-Benharira et al., 2006; Lopez et al., 2009; Bridle et al., 2010; Polechová, 2018), the type of density regulation (Holt, 1996, 1997; Gomulkiewicz et al., 1999; Filin et al., 2008), species interactions (Case & Taper, 2000; Tufto, 2001; Gandon & Michalakis, 2002; Nuismer & Kirkpatrick, 2003; Case et al., 2005; Nuismer, 2006; García-Ramos & Huang, 2013; Urban et al., 2019), phenotypic plasticity (Sasaki & de Jong, 1999; Chevin & Lande, 2011), the genetic

architecture of adaptive traits (Kawecki, 2000; Kimbrell & Holt, 2007; Schiffers et al., 2014; Gilbert & Whitlock, 2017) or dispersal (Ronce & Kirkpatrick, 2001; Kawecki, 2003; Aguilée et al., 2016). How populations living in such landscapes will, on top of that, respond to a progressive deterioration of their environment, may be even more difficult to predict.

There has been an appreciation in the past two decades that eco-evolutionary dynamics can unfold on short, ecological time scales (Kinnison & Hairston, 2007; Hendry, 2017), thus begging the question of the potential of natural populations for evolutionary rescue (the phenomenon by which a population or species avoids extinction through genetic adaptation, Kinnison and Hairston, 2007; Bell and Collins, 2008; Gonzalez et al., 2013; Bell, 2017) in the face of climate change. Earlier work focusing on simple scenarios of environmental change highlighted the now well-accepted roles of genetic variation, speed of environmental change, population size and stochastic demographic effects in adaptation to a changing climate (Levins, 1974; Pease et al., 1989; Holt, 1990; Bürger & Lynch, 1995; Gomulkiewicz & Holt, 1995; Boulding & Hay, 2001; Gomulkiewicz & Houle, 2009; Willi & Hoffmann, 2009; Holt & Barfield, 2011; Arenas et al., 2012; Polechová & Barton, 2015). Moreover, theoretical models have confirmed that many of the factors influencing local adaptation should also impact evolutionary rescue, such as genetic architecture (Orr & Unckless, 2008; Gomulkiewicz et al., 2010; Duputié et al., 2012; Schiffers et al., 2014), recombination (Uecker & Hermisson, 2016), dispersal (Alfaro et al., 2017) or species interactions (Case & Taper, 2000; Mellard et al., 2015). Yet, most of the studies done so far do not consider adaptation to a changing climate in conjunction with a population that already inhabits a heterogeneous landscape, such as a plant community subject to interspecific ecological facilitation.

Here, we aim to address this gap with a theoretical study of adaptation to climate change in a facilitated sessile species living in a stressful, heterogeneous environment, with (facilitated) sheltered and (unfacilitated) hostile patches, as the conditions in this environment deteriorate. Our study is inspired by the case of *Brachypodium distachyon*, an annual grass species found in semi-arid ecosystems across the Mediterranean basin, and often found in natural populations in a facilitative association with nurse shrubs, underneath which *B. distachyon* plants are found to be taller and have higher seed production than grasses growing in the open landscape (Korte et al., 2025). These phenotypic differences between plants growing in facilitated and unfacilitated environments were also found to be retained over several generations in greenhouse experiments (Korte, 2024), indicating that nurse shrubs do affect fitness traits in spatially associated *B. distachyon* and could play a role in local adaptation in this species. While our modeling is inspired by plants, the results of our study could in principle extend more generally to other organisms experiencing ecological facilitation, as long as they are sessile (e.g. in marine systems, Bulleri, 2009, or soil mycorrhizal networks, van der Heijden and Horton, 2009).

We developed a model where our focal species lives and evolves in a heterogeneous landscape composed of facilitated and unfacilitated patches (mimicking a semi-arid ecosystem with areas covered by nurse shrubs and open landscape). Note that unfacilitated patches are not just

another niche in this landscape, where fitness can be optimized to the same level as in the facilitated patches through some locally optimum phenotype. Instead, the conditions in the harsh matrix outside of the shrubs are inherently limiting and close to the physiological limits of the organism (similar to sinks sensu Kawecki, 2008; Chevin and Hoffmann, 2017). Survival in these patches requires (genetically determined) investment in stress tolerance, which comes at a fecundity cost, and the carrying capacity (i.e. the population density that can be sustained) is low compared to the less limiting facilitated patches, for an area of the same surface. Using a combination of individual-based simulations and adaptive dynamics analyses (Metz et al., 1992, 1996; Geritz et al., 1998), we study the eco-evolutionary dynamics and equilibrium states reached by our facilitated population in such a landscape, as well as its resilience and potential for adaptation to different scenarios of habitat deterioration driven by climate change. We expand our results to different numbers of heterogeneous demes in a metapopulation setting, and to various levels of outcrossing (an important modulator of the effects of recombination in annual plants, Pannell, 2016) versus selfing (i.e. self-fertilization).

Methods

The model

We consider a landscape consisting of n_D demes, or *sites*, each containing two habitat *patches* (Fig. 1A) — a facilitated patch (F), and an unfacilitated patch (UF). The facilitated patch represents the total area of the site that is covered by nurse shrubs. The unfacilitated patch represents the area that is not protected. Although facilitated patches would typically correspond to individual shrubs in a semi-arid landscape and therefore be patchy, here we clumped all shrubs together within each site. We assume this is a reasonable simplification, reflecting that shrub locations may be labile on an evolutionary time scale, and may be more accurately described as a general cover that applies to the whole site. Hence, each site k is characterized by its fractional cover c_k in facilitated patches (the area of the site that is unfacilitated is $1 - c_k$).

A population of individual grasses dwells in this landscape. Every generation, each adult plant produces a number of seeds, or offspring, sampled from a Poisson distribution with a mean that is equal to the expected reproductive output of that parent plant. The reproductive output of a plant is a function of its stress tolerance, which may be regarded as its resistance to aridity, and of local density dependence arising from competition with other plants living in the same local patch. For a plant living in patch j (UF or F) of deme k and with stress tolerance level x, we assume that this reproductive output is given by

$$r_{jk}(x) = \exp\left[y(x) \left(1 - \frac{N_{jk}}{C_{jk} K_j} \right) \right] \tag{1}$$

where N_{jk} is the number of plants in patch j of site k, C_{jk} is the shrub cover in that patch (equal to c_k if $j = $ F and $1 - c_k$ if $j = $ UF), K_j is the per-area carrying capacity of patch j (the same across all demes, as it roughly represents the number of individuals that a given surface of bare or covered soil can sustain), and y is the fecundity, given by

$$y(x) = r_{max} - \epsilon x \left(x/x_{max} \right)^{\nu - 1} \tag{2}$$

where r_{max} is the maximum achievable population growth rate, x_{max} is the maximum achievable stress tolerance level, ϵ is a trade-off parameter incurring a fecundity cost to higher stress tolerance, and ν is a non-linearity parameter modifying the shape (convex for $\nu < 1$, linear for $\nu = 1$ or concave for $\nu > 1$) of the trade-off relationship between stress tolerance and fecundity (Fig. 1B) — an aspect which may have important consequences on the dynamics of an evolving system under selection (e.g. de Mazancourt and Dieckmann, 2004). Note here that stress tolerance x not only affects the (density-independent) fecundity $y(x)$, it also indirectly affects the density-dependent part of the reproductive output $r_{jk}(x)$ because of its effect on the number of individuals, N_{jk}, able to coexist given the local carrying capacity.

Fertilization   Many plants can self-pollinate as well as outcross. In the annual grass *Brachypdium distachyon*, for example, the rate of outcrossing is thought to be about 5% (Vogel et al., 2009). In the model, each seed produced by an adult plant can either result from fertilization by pollen

from another plant with outcrossing probability g, or from selfing, with probability $1-g$. If a seed is the result of outcrossing, one plant is chosen at random from the entire population (i.e. from any deme) to be the provider of the fertilizing pollen grain (all plants being hermaphrodites). This reflects the assumption that pollen is small enough that long-range dispersal is readily achieved.

Dispersal   Once fully formed, each seed can disperse to another site with probability m, the migration rate (Fig. 1A). Within a site, each seed lands into a patch with probability proportional to the surface of that patch in that site (c_k for F or $1 - c_k$ for UF). This free dispersal of seeds within sites, but not between sites, reflects the assumption that seeds are more likely to land meters away from their parent plant (possibly in a different microhabitat), while long-range dispersal to far away sites is less likely (Korte, 2024).

Germination   Upon landing, the survival and successful germination of each seedling is sampled with a probability that depends on the level of stress tolerance x of that seedling, relative to the intensity of the stress it encounters in its local patch. The survival probability of a seedling in patch j and in site k is assumed to be given by the decreasing sigmoid function,

$$s_{jk}(x) = \frac{1}{1 + \exp\left[a\left(\theta_{jk} - x\right)\right]} \tag{3}$$

in which the probability of survival decays from one to zero as the stress level of the environment θ_{jk} increases relative to the tolerance level x of the plant, a being the magnitude of the downward slope of the sigmoid at its inflection point (where $\theta_{jk} = x$ in Fig. 1C). This means that stress tolerance x must be somewhat larger than environmental stress θ_{jk} for the seedling to have somewhat decent chances of survival (Fig. 1C).

Genetics   Stress tolerance is encoded by a number of separate loci in the genome. We assume that each plant has a haploid genome consisting of $n_{\mathrm{L}} = 100$ loci, uniformly distributed along a single chromosome (the genomic position of each locus is the same for all individuals, and is randomly sampled at the start of a simulation). Within an individual, each locus can harbor either of two alternative alleles, a *stress-sensitive* allele (0) and a *stress-tolerant* allele (1) (Fig. 1D). The level of tolerance (i.e. the phenotype) of a plant is equal to the sum of the contributions of all alleles in its genome, where each tolerance allele contributes a quantity η, the locus effect size (which is the same for all loci unless stated otherwise) to the final tolerance value (Fig. 1D).

Once a seed is fertilized, genetic recombination occurs between the two parental genomes. Upon recombination, the genome of the offspring is a haploid result of a series of crossovers between the two parental haplotypes, where crossover points are sampled at an exponentially distributed distance from each other with rate ρ, the recombination rate. The genome of the seed is randomly picked among the recombinant haplotypes produced by this meiosis process. Because the genome is haploid, self-fertilization is equivalent to asexual (i.e. clonal) reproduction. Hence, in the model, if a seed is not the result of outcrossing, it simply inherits the haplotype of its (maternal) parent plant. Each locus within the offspring then mutates with

7

probability μ, the mutation rate, which flips the allele present at that locus to its opposite (0 becomes 1 and vice versa).

At the end of each discrete generation, all adult plants die (the species is an annual) and the seedlings that have survived become the adults of the next generation. Every simulation is initialized with a population of N_0 individuals whose genomes are randomly generated with initial frequency p_0 for the tolerance allele. All founder individuals are randomly scattered across the landscape, with equal probability to land in each site, but landing in each patch with probability proportional to the relative surface of that patch (c_k or $1 - c_k$) in the local site. Table 1 summarizes the model parameters and their default values.

Simulations

We ran individual-based stochastic simulations of our model, first to understand its dynamics and evolutionary outcomes across parameter combinations, and subsequently to study the potential for evolutionary rescue of a facilitated population in the face of climate change. For that latter purpose, we designed a digital 'climate change experiment' in which we subjected the population to different scenarios of environmental deterioration (by means of progressively changing environmental parameters through time, see below).

Null scenario In what follows, we first examine the dynamics and evolutionary steady states of the model, in conditions most relevant to our study system (facilitation by nurse shrubs in a harsh matrix). These conditions are: higher stress levels in unfacilitated compared to facilitated patches ($\theta_{\mathrm{UF}} > \theta_{\mathrm{F}}$), and much lower carrying capacities per surface area ($K_{\mathrm{UF}} \ll K_{\mathrm{F}}$).

Climate change experiment Each simulation in the experiment started with 10 000 generations of evolution in a constant environment resembling typical semi-arid, facilitated-landscape conditions. We then subjected the population to one of three climate change scenarios. In the first scenario (stress increase under the shrubs), we increased the level of stress θ_{F} and decreased the carrying capacity K_{F} of the facilitated patch until these two parameters reached the values of the unfacilitated patch (θ_{UF} and K_{UF}, respectively). In the second scenario (whole-landscape deterioration), we increased the stress level and decreased the carrying capacity of the facilitated patches (θ_{F} and K_{F}) as well as of the unfacilitated patches (θ_{UF} and K_{UF}). In the third scenario (shrub-cover shrinkage), stress level and carrying capacity remained unchanged but we reduced the shrub cover c. The exact values of the varied parameters are given in Table 2. All changes in parameters were gradual and linear through time (Fig. 2). The three scenarios correspond to different ways in which global warming may affect the system. For each scenario, we explore the effect of various rates of environmental change Δt_{W} (or warming period, i.e. the number of generations needed for environmental parameters to reach their final value).

Adaptive dynamics

Separately from the stochastic simulations, we developed a deterministic approximation of the model, which we study here using adaptive dynamics theory (Metz et al., 1992, 1996; Geritz et

al., 1998), to tease apart the role of selection from that of genetics or stochasticity in simulation outcomes. These analyses and accompanying derivations are detailed in the Appendix, and notably allow to determine whether and under which conditions plants of different morphs (i.e. with different tolerance strategies) can diversify within the model. However, because coexistence does not rely exclusively on evolutionary diversification in situ, the scope for the maintenance of polymorphism is wider than for sympatric divergence only. In this study, to map the portions of parameter space where such coexistence of two morphs is permitted, we perform *mutual invasibility analyses* based on our adaptive dynamics approximation (Geritz et al., 1998). These analyses consist in establishing first, for a given parameter combination, which pairs of strategies are capable of mutually invading each other (therefore, of coexisting as part of a protected polymorphism). Once pairs of morphs are found that can potentially coexist, we ask, for each pair, whether evolution will maintain this coexistence (if so, they form a *stable coalition*). To perform this type of analysis, we derived equations for the selection dynamics in a system with two morphs (see Appendix). We then use these equations to predict, for all putative pairs of coexisting morphs, which would evolve towards a stable equilibrium coalition where two morphs are still present (i.e. where none has outcompeted the other), and what their phenotypes would be. Figure S2 illustrates the analysis graphically.

Specifications

The simulation code in this study was written in the programming language C++20 using standard libraries. Analyses of the simulations were performed in the R computing language, version 4.3.3 (R Core Team, 2025). Adaptive dynamics calculations were performed in R and in C++. See accompanying code for details.

Results

Constant climate

Under stable semi-arid conditions, either of two possible alternative strategies can generally evolve in our simulations. The first strategy is a *stress-sensitive* strategy, whose stress tolerance value is just above the level of stress occurring in facilitated patches, but well below that of the unfacilitated patches (Fig. 3A, red circle). Consequently, plants with this strategy can only survive in the facilitated patches (Fig. 3C). The second strategy is a *stress-tolerant* strategy, whose stress tolerance is just above the level of stress of the unfacilitated patch (Fig. 3A, blue circle). This strategy can survive in both the unfacilitated and the facilitated patches (Fig. 3C).

These two alternative outcomes result from a balance between selection favoring adaptation to the stressful conditions of the unfacilitated patches, and the fecundity costs of increased stress tolerance (which trades off with reproductive output, see Eq. 2). On the one hand, if we remove stress in the unfacilitated patches, only a sensitive morph is predicted to evolve (see e.g. Fig. S3, $\theta_{\mathrm{UF}} = 0$). On the other hand, if we remove the fecundity cost to stress tolerance ($\epsilon = 0$), selection favors ever-increasing adaptation to stress (see e.g. Fig. S4). Shrub cover plays a role too, as the tolerant strategy remains the only possible outcome if the shrub cover is too low to support a viable population of the sensitive morph (see e.g. Fig. S5, $c = 0.1$).

Under the aforementioned conditions, the stress-sensitive and stress-tolerant strategy represent alternative stable states of the system: both are stable attractors of the evolutionary dynamics, but with distinct and exclusive basins of attraction. Which strategy the population evolves towards depends on its starting stress tolerance (determined by the initial allele frequency p_0). If the starting stress tolerance value is below a certain threshold (the border between basins of attraction in Fig. 3A), the population evolves towards the sensitive strategy, and therefore only establishes underneath the nurse shrubs (low p_0 in Fig. 3B–C). If the initial stress tolerance is above that point, the population evolves into a stress-tolerant morph capable of establishing inside and outside the shrubs (high p_0 in Fig. 3B–C).

The survival of a facilitated population in a harsh environment that can no longer sustain a stress-sensitive strategy depends on the evolution of a stress-tolerant strategy that no longer relies on facilitation from nurse shrubs. A population starting off as highly stress sensitive will rapidly go extinct, for example, in an environment where the shrub cover is too low for this population to be viable (e.g. $c = 0.1$ in Fig. S6). Increasing the rate of outcrossing g does not rescue the population from extinction in such environment (Fig. S6B).

Outcrossing In some cases, outcrossing can make the difference between survival and extinction of a stress-sensitive population in a constant climate. This happens in conditions that are not so harsh that the sensitive strategy is totally nonviable, but harsh enough that only low densities of sensitive plants can be sustained, which would otherwise go extinct due to stochastic demographic fluctuations if only selfing occurs ($g = 0$, Fig. S7). The rescue effect of outcrossing

10

is likely due to an increase in genetic variance through recombination, improving the efficiency of selection in homogenizing phenotypic values around the sensitive equilibrium strategy, and avoiding genetic drift into neighboring areas of phenotype space with dangerously low equilibrium densities (which causes extinction in selfing populations, Fig. S7E–G). Note that because of demographic stochasticity, this effect of outcrossing is only visible when the total population size is high enough (e.g. $n_D = 5$ in Fig. S7B).

Climate change experiment

In our climate change experiment, we first evolved an initially stress-sensitive population in similar conditions as described above, i.e. resembling a patchy semi-arid landscape, for 1 000 generations. We then changed certain environmental parameters, gradually and at different paces, according to three different scenarios (see Methods).

Scenario 1: stress increase under the shrubs   In this scenario, the level of stress θ_F and the carrying capacity K_F of the facilitated patch were increased and decreased, respectively, until these two parameters reached their corresponding values θ_{UF} and K_{UF} in the unfacilitated patch. We find that a population readily survives the changing climate (as long as the pace of climate change is not too fast) by evolving a higher stress tolerance, thus adapting to the conditions in the open landscape as the environment underneath the shrubs becomes more and more similar to that on the outside (Fig. S8A, S9A). A look at the adaptive dynamics of this scenario shows that out of the two possible evolutionary equilibria, the stress-sensitive strategy quickly becomes nonviable as the climate deteriorates (i.e. as θ_F and K_F change throughout the experiment), and only the stress-tolerant equilibrium strategy remains, as sole attractor of the evolutionary dynamics, for the rest of the simulation (Fig. 4A).

Scenario 2: whole-landscape deterioration   In this scenario, the stress level was increased, and the carrying capacity decreased, in both the facilitated and unfacilitated patches. Here we often find extinction (Fig. S8B, S9B) where the population initially evolves higher stress tolerance (Fig. S9B), but eventually becomes extinct nonetheless, regardless of the pace of environmental change. The adaptive dynamics of this scenario reveal that as the stress tolerance of the population increases, so does the minimum level of stress tolerance needed to survive outside the shrubs (Fig. 4B). Limiting the change in conditions outside of the shrubs (the final values of θ_{UF} and K_{UF}, thus bringing the simulation closer to the first scenario, Fig. S10), as well as increasing the mutation rate μ (Fig. S11A), both help rescue the population from extinction. Furthermore, the slower the deterioration of the unfacilitated patches, the lower the minimum mutation rate needed to rescue the population (Fig. S12). This suggests that extinction has more to do with the distance to the viable stress-tolerant strategy in phenotype space than with the speed of environmental change per se.

Scenario 3: shrub-cover shrinkage   In this scenario, stress level and carrying capacity stayed constant and the shrub cover c (i.e. the surface occupied by the facilitated patches) was reduced instead. Here we invariably find extinction, irrespective of the pace of shrub

11

cover loss (Fig. S8C, S9C). However, contrary to the second scenario, in this scenario the population does not evolve higher stress tolerance before going extinct. Instead, its stress tolerance remains more-or-less stable (Fig. S9C). Using adaptive dynamics analysis, we find that the population is trapped in a portion of phenotype space, centered around the stress-sensitive strategy that is viable under the shrubs, but shrinking in phenotypic width, and from which the population is unable to escape once that window closes and low stress tolerance becomes nonviable (Fig. 4C). Population survival in this portion of phenotype space depends on the shrub cover being just high enough to maintain a viable population of plants without stress tolerance, and remains possible as long as the stress level in the facilitated patch is low (which it is in our scenario, Fig. S13). A population trapped in this portion of phenotype space cannot escape extinction, however, because at the moment when the shrub cover has become too low to support a population of stress-sensitive plants, the boundary of extinction (i.e. the lowest stress tolerance allowing to survive in the unfacilitated patches) has gone up so far that it has now become unreachable through small mutational steps from a sensitive strategy (Fig. 4C). Consistent with that, allowing for a few macromutations (giving some loci in the genome particularly high effect sizes, Fig. S8D and S9D) or simply increasing the mutation rate (Fig. S11B), both allow to rescue the population from shrinking shrub cover.

Outcrossing Outcrossed populations generally evolve a stress-tolerant strategy slightly earlier than selfing populations in the scenario with stress increase under the shrubs (Fig. S14, left panel). Moreover, outcrossing can also rescue populations from extinction in the whole-landscape deterioration scenario (middle panel) and in the shrub-cover shrinkage scenario (right panel), but only when the rate of climate change Δt_W is slow and outcrossing is high (e.g. from $g = 0.3$ in the whole-landscape deterioration scenario, and from $g = 1$ in the shrub-cover shrinkage scenario in Fig. S14). This can be explained by the increase in phenotypic variance brought about by recombination when plants reproduce sexually (see e.g. Fig. S7E), which increases the probability that the population escapes its evolutionary attractor and falls within the phenotypic vicinity of the stress-tolerant equilibrium strategy (similar to the effect of introducing macromutations, Fig. S9D, or increasing the mutation rate, Fig. S11).

Number of demes Because of its effect on total population size, increasing the number of demes in the metapopulation delays extinction by thousands of generations in the whole-landscape deterioration and shrub-cover shrinkage scenarios, and prevents rapid extinction in the scenario with stress increase only under the shrubs, when climate change is otherwise too fast for a single deme to adapt (Fig. S15). In contrast, more demes in the specific case of the shrub-cover shrinkage scenario with maximum outcrossing ($g = 1$) actually accelerate extinction, where a single deme would otherwise be rescued by outcrossing (Fig. S15, see previous section on the role of outcrossing and Fig. S14). This suggests that while recombination may rescue the population from extinction in a single deme when the shrub cover shrinks, in combination with migration among demes, gene flow may instead homogenize phenotypes, preventing any one deme from undergoing the relatively rare event of evolving away from the (soon-to-become nonviable) stress-sensitive equilibrium strategy.

12

Divergence in sympatry

In our model, evolution can lead to either a stress-sensitive or a stress-tolerant strategy, and under some conditions both strategies can coexist. The diversification of both strategies from a single one occurs when the tolerant strategy becomes an evolutionary *branching point*, allowing a sensitive morph to diverge and persist alongside it (Fig. S16 and S17). Branching arises when the carrying capacity of unfacilitated patches is sufficiently low that frequency-dependent selection favors the evolution of sensitive plants that can enjoy a fecundity advantage under the shrubs, without outcompeting the tolerant morph that still retains a higher survivability over the landscape. By contrast, populations starting from a sensitive strategy never branch, since their higher fecundity prevents tolerant mutants from establishing. Overall, branching requires facilitated patches to host roughly an order of magnitude more individuals per unit area than unfacilitated patches (Fig. S18). Figure S19 summarizes the conditions under which branching may happen. Note that since the climate change experiment always started with sensitive plants, branching points were never encountered there. See Supplementary Results S1 for a more detailed explanation.

Maintenance of diversity

Coexistence between sensitive and tolerant strategies does not rely solely on sympatric branching. It can also arise through secondary contact in a metapopulation ($n_D > 1$), where strategies that evolved separately become able to persist together (Fig. S20). Using mutual invasibility analysis (see Methods, Fig. S2), we show that stable coexistence is possible across a broader parameter space than predicted from branching alone (Fig. S21, S22), suggesting that migration among sites should play a key role in maintaining local diversity, as in its absence, it cannot be regained once lost without a branching point. However, sexual reproduction and gene flow often disrupt this diversity in the long term in the absence of mechanisms like assortative mating or reproductive isolation (Fig. S23). See Supplementary Results S2 for details.

Non-linear trade-offs

We varied the shape of the trade-off function between survival and fecundity by means of the non-linearity parameter ν, which could make the trade-off curve more convex ($\nu < 1$) or concave ($\nu > 1$), on top of the main trend imposed by the trade-off strength parameter ϵ (the downward slope of the linear trade-off when $\nu = 1$, Eq. 2, Fig. 1C). Changing the shape of the trade-off curve does not greatly affect the conclusions we derived from a linear version of the model. Qualitatively, the same kinds of evolutionary steady states are found in the same portions of parameter space (Fig. S24). The non-linearity parameter mostly acts as a modifier of the effect of the linear trade-off strength on the adaptive dynamics of the system, increasing the impact of the trade-off when convex, and dampening it when concave (Fig. S25).

13

Discussion

Climate change is negatively affecting terrestrial ecosystems worldwide, especially those that occur in water-restricted regions (IPCC, 2014). Shrub-dominated landscapes, like those found in the Mediterranean basin, provide habitat heterogeneity which results in buffered refuges for spatially associated plant species. This relegates facilitation into an integral component of the adaptation and survival of species in the face of climate change (Tirado & Pugnaire, 2003; Brooker, 2006; Lortie et al., 2022). Here, we used a modeling approach to gain insights into the eco-evolutionary consequences of ecological facilitation on resilience to climate change in an annual grass, inspired by the species *Brachypodium distachyon* (a study system for interspecific facilitation, Korte et al., 2025), in a semi-arid landscape, or more generally, in a heterogeneous landscape with mild and harsh patches.

By performing a digital climate change experiment in which we exposed a population of individuals experiencing facilitation from nurse shrubs to various scenarios of environmental degradation, we find the following. First, a population will evolve higher stress tolerance, and become less dependent on nurse benefactor shrubs, if climate change incurs a change in *quality* of the facilitated areas, that is, an increase in stress (e.g. aridity or reduction in nutrient content) under the shrubs, making it more difficult for seedlings to germinate and reducing the carrying capacity (the density of plants that can be sustained per unit area) in those protected patches. In other words, if biologically feasible, plants will adapt to life outside of the shrubs if the conditions underneath the shrubs become more similar to those outside. Extinction may still happen if this change is too fast and/or if the unfacilitated areas deteriorate faster than the genetic variance of the population allows it to keep up with. Second, a reduction in the *quantity* of facilitated patches (i.e. shrub cover), without a change in quality of such patches, almost invariably leads to extinction, as short-term selective advantage traps the population in a facilitation-dependent state. The population remains restricted to the receding shrubs until the shrub cover has become too low for a viable population of grasses to be sustained — at that point the phenotypic jump that would be needed to rescue the population and allow it to survive in the open landscape has become so large that it will in practice not occur with small mutational steps (i.e. large-effect mutations or a substantial inflow of genetic variance would be needed). This is not simply a consequence of the removal of a niche from the landscape, but a result of selection dynamics that can be explained by frequency dependence. As long as the shrubs are present, they offer a refuge for plants that do not invest in stress tolerance, which, if stress tolerance incurs a fecundity cost, outcompete slightly more stress-tolerant mutants (even though high stress tolerance may be the better option overall), thus preventing them from arising. Selection for short-term benefit keeps the population in a state in which extinction becomes unavoidable when shrub cover decreases beyond a certain threshold.

Studies of the impact of ecological facilitation on evolutionary dynamics are relatively scarce. Using simulations, Kéfi et al. (2008) showed that a self-facilitating plant may drive itself to extinction during landscape aridification, if cheaters investing less in facilitation invade the system. Liancourt et al. (2012) propose that facilitation slows down adaptation to harsh environments

14

because of maladaptive gene flow and hybrid rescue. Yet other modeling studies have focused on the eco-evolutionary dynamics of the benefactor rather than the beneficiary species (Michalet et al., 2011). In our study, we show that contrary to Kéfi et al. (2008) where it is the loss of facilitation that leads to extinction, the maintenance of facilitation from an external benefactor species can also prevent a population from adapting to harsher conditions. However, unlike the argument proposed by Liancourt et al. (2012) and reminiscent of the literature on adaptation at range edges (e.g. Kirkpatrick and Barton, 1997; Lenormand, 2002; Bridle et al., 2010; Angert et al., 2020), we show with asexual simulations that maladaptive gene flow is not necessarily the culprit, and that the dynamics of frequency-dependent selection may be at play instead (stress-sensitive plants take up some of the carrying capacity of the unfacilitated patches, thereby outcompeting slightly more stress-tolerant mutants with lower fecundity).

Another explanation that has been put forward for the difficulty of adaptation to harsh habitats in heterogeneous landscapes is that of weaker selection in demographic sinks, where fitness and density are lower (Kawecki, 1995; Kawecki & Holt, 2002; Holt et al., 2003; Kawecki, 2008). However, this stems from the population-genetic argument that a beneficial allele will increase in frequency more slowly because of a stronger effect of drift. Although this effect probably occurs in our stochastic individual-based simulations, using adaptive dynamics theory (which ignores drift and purely evaluates the effect of selection, Metz et al., 1996), we show that selection itself, independently of drift, will also prevent the invasion of mutants investing slightly more in stress tolerance. This is because of a frequency-dependent competitive advantage not to suffer the fecundity cost of investing in more stress tolerance, at least as long as sufficient shrub cover (i.e. facilitation) remains. Hence, we propose that on top of (1) maladaptive gene flow and (2) weaker selection relative to drift, (3) frequency-dependent selection arising from the life history trade-off between survival and fecundity also explains why heterogeneous environments with facilitated patches may have a deleterious effect on adaptation to harsher conditions. Elucidating the relative importance of these forces may constitute a fruitful avenue for further research.

A key parameter that commonly differs among plant species is their rate of outcrossing versus selfing (Pannell, 2016). The rate of outcrossing is thought to influence the adaptive potential of a species because of the direct impact of recombination on genetic diversity, and its ability to bring beneficial alleles onto the same haplotype (Tufto, 2001; Uecker & Hermisson, 2016). We find that outcrossing can make the difference between life and death in situations where the population is dangerously close to its extinction boundary, for example, when the environment favors a stress-sensitive strategy, but one that can only remain at very low densities. In such cases, outcrossing counteracts the high risk of drift into phenotypes whose survival and/or fecundity bring the population growth rate below one. The opposite effect is found, however, in a metapopulation setting, where the same homogenizing effect of recombination associated with gene flow prevents any one deme from stumbling upon a sufficiently stress-tolerant phenotype, which could eventually rescue the entire metapopulation once facilitation disappears from the landscape.

Phenotypic plasticity can be an alternative to genetic adaptation in surviving to a changing climate (Chevin et al., 2010; Chevin & Hoffmann, 2017). In our implementation the more stress tolerant plants can survive both underneath the shrubs and outside — we do not model how this stress tolerance materializes explicitly, but it could well correspond to some plastic change in key phenotypes directly related to water uptake, retention and loss (such as leaf area or root biomass), depending on where the stress-tolerant plant grows. In contrast, a stress-sensitive plant could be seen as a plant unable to plastically modify its metabolism depending on external stress. Hence, our model technically describes the evolution of plasticity, if stress tolerance is to be interpreted as a form of genetically encoded plasticity that comes at the cost of fecundity.

The validity of our results rests on their applicability to the real world. One of our assumptions was that of implicit space, where we clumped all nurse shrubs together in a single facilitated habitat patch per deme, instead of modeling individual nurse shrubs in a spatially explicit context (e.g. as in Kéfi et al., 2008; Michalet et al., 2011). This approach has the advantage of helping disentangle the impact of habitat heterogeneity brought about by facilitation from the dynamics of the benefactor species. However, while it may be a reasonable assumption when considering that the specific location of nurse shrubs may be labile over evolutionary time, and a general cover may be sufficient to capture the facilitated part of the landscape, studying a spatially explicit version of this model, with eco-evolutionary dynamics of the benefactor as well as the beneficiary species, seems a logical next step. Additional factors could then be explored too, such as specific assumptions about the evolutionary investment into facilitation by the benefactor species (e.g. as in Kéfi et al., 2008), the evolution of dispersal (Ronce & Kirkpatrick, 2001; Holt et al., 2003; Ronce, 2007), or more complex and evolving genetic architectures than the polygenic additive genetics used here (e.g. while capable of harboring cryptic genetic variation and generating large mutational steps, Crombach and Hogeweg, 2008; Paaby and Rockman, 2014, gene networks can hinder adaptation to new patches in heterogeneous landscapes by favoring genetic canalization, Kimbrell and Holt, 2007). Habitat choice and sexual selection may be factors to consider too (Holt, 1985; Proulx, 2002), although less relevant in sessile organisms. Similarly, the effect of hybridization with closely related species could also be investigated (as it may affect the potential for local adaptation, Kawecki, 2008), especially in the case of *B. distachyon*, which is commonly found to coexist with its more stress-tolerant congeneric relative, *Brachypodium hybridum* (Korte, 2024).

Global climate change is occurring within a relatively short time frame and plant communities are especially vulnerable. Investigation of the eco-evolutionary dynamics of biotic interactions such as facilitation can help gain insight into mechanisms that could drive local adaptation and its subsequent effect on plant community dynamics. Bridging the gaps between ecological and evolutionary theory can shed light on the conditions that could help mitigate the effects of current environmental stressors that could otherwise result in significant declines, or even extinction, of certain plant populations. Here, we used theoretical modeling tools to help bridge that gap, and show that the evolutionary fate of a species facing the risk of ex-

tinction in a facilitated landscape crucially depends on the way in which climate change affects the environment — with receding facilitated patches almost invariably leading the population to extinction, while exposing the population to deteriorating conditions in the facilitated areas readily promotes adaptation. This showcases how theoretical models reveal the mechanisms at play in the eco-evolutionary dynamics of species facing climate change, and the factors that may be key in predicting the response of organisms. Future work could use our model to tailor to specific study systems and produce quantitative predictions for the conservation of species of particular interest.

Acknowledgments

Author Contributions

RS and MK conceived the study. RS developed the simulation code, performed the analyses, and wrote the first draft of the manuscript. MK contributed to study design and interpretation of the results and, together with GSvD and RSE, provided critical feedback on the manuscript. GSvD and RSE provided additional feedback on mathematical analyses.

Tables

Table 1: Parameters used in this study and default values. Unless mentioned otherwise, the values of parameters being kept constant are as per this table. See Appendix for details on the deterministic approximation model.

Symbol	Parameter	Default
n_{D}	Number of demes	1
c_k	Shrub cover in site k	0.5
θ_j	Environmental stress in habitat j	$\{5, 0\}$
K_j	Carrying capacity per unit area in habitat j	$\{500, 2\,000\}$
r_{max}	Maximum population growth rate	2
a	Steepness of the stress tolerance function at inflection	5
g	Rate of outcrossing	0
m	Rate of dispersal	0.0001
n_{L}	Number of loci	100
p_0	Initial allele frequency	0.5
μ	Mutation rate	0.0001
η	Effect size of a locus	0.1
ϵ	Trade-off between survival and fecundity	0.1
ν	Non-linearity of the trade-off curve	1
x_{max}	Maximum possible stress tolerance	10
	Climate change experiment	
Δt_{W}	Duration of the warming period	20\,000
	Deterministic approximation model	
μ_x	Phenotypic mutation rate	0.01
σ_x	Mutational standard deviation	0.5

Table 2: Change in environmental parameters in our climate change experiment. See Table 1 for details about parameters.

Scenario	Parameter affected	Starting value	End value
Stress increase under the shrubs	θ_{F}	0	5
	K_{F}	2 000	100
Whole-landscape deterioration	θ_{F}	0	5
	θ_{UF}	5	7
	K_{F}	2 000	100
	K_{UF}	100	50
Shrub-cover shrinkage	c	0.3	0.1
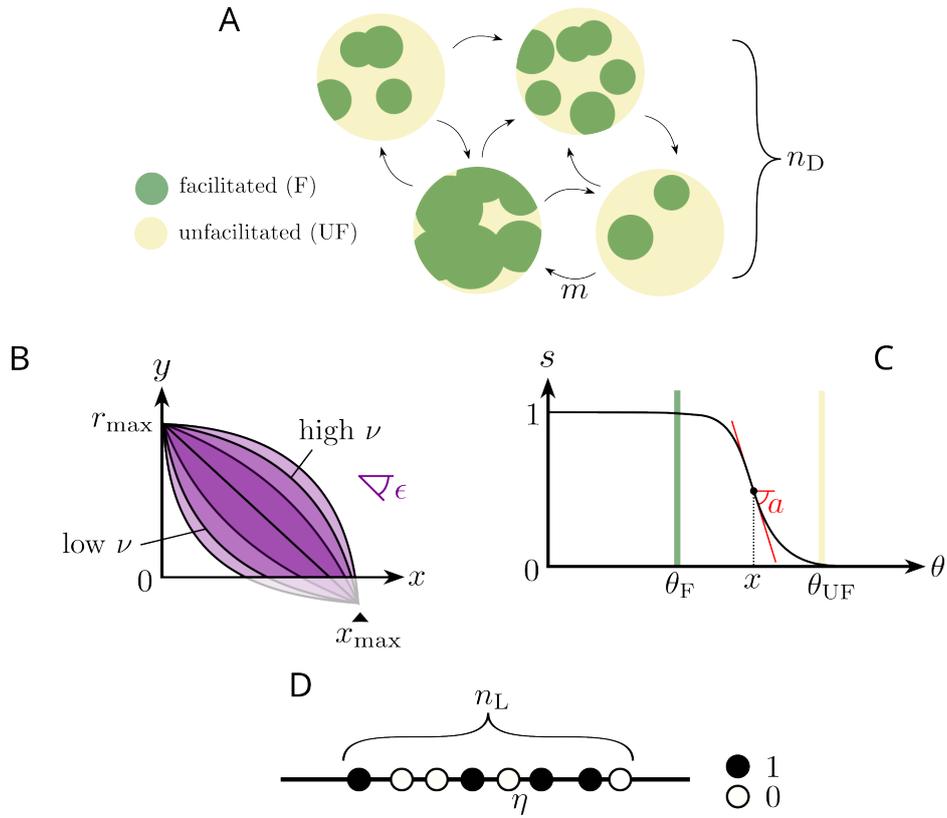
Figures

Figure 1: Model overview. (A) Schematic representation of the landscape, consisting of n_{D} demes, or sites, each covered by a certain area of shrubs (the *facilitated* patches, or F) and the rest being relatively arid and unsheltered (the *unfacilitated* patches, or UF). Migration occurs at rate m between the sites. (B) The trade-off between stress tolerance x and reproductive output y. The strength of this trade-off is determined by its slope, $-\epsilon$, and its shape by the non-linearity parameter ν. (C) The sigmoid relationship between survival s and environmental stress θ. Once environmental stress goes beyond the tolerance capacity of the plant (the inflection point x), the chances of survival are drastically reduced (depending on the steepness a of the survival curve). In this example, the focal plant is tolerant enough to survive in the facilitated patch ($x > \theta_{\mathrm{F}}$) but is likely to die in the unfacilitated patch ($x < \theta_{\mathrm{UF}}$). (D) The genome consists of n_{L} loci in either state (or allele) 0 or 1, where 1-alleles contribute an effect size η to the stress tolerance x of the individual. See Table 1 for default parameter values.
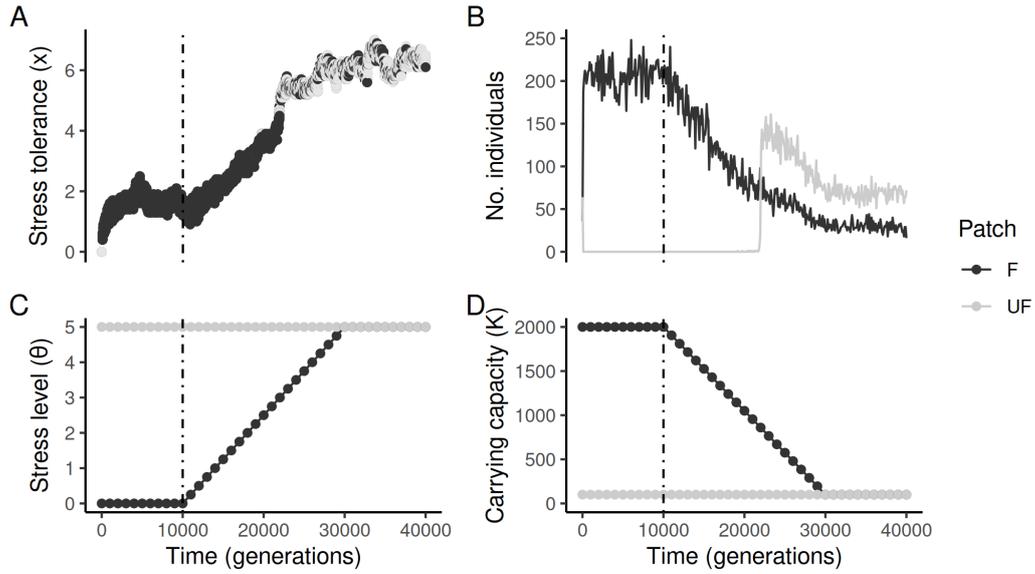
Figure 2: Typical setup for our climate change experiment. In this example, the population first evolves for 10 000 time steps in a stable environment. Relevant climate-dependent parameters (here, the stress level θ_F and carrying capacity K_F in facilitated patches) start changing at time step 10 000, and reach their final value after Δt_W time steps. (A) Stress tolerance values of all individuals through time (colored by patch where the individual lives). (B) Densities of individuals in each patch through time (in this example there is only $n_D = 1$ deme). (C) Stress levels θ_F and θ_{UF} through time. (D) Carrying capacities K_F and K_{UF} through time. Parameter values in this example are as per Figure 3, except with $c = 0.3$ to reflect a semi-arid environment in which nurse shrubs occupy less than half of the entire landscape.
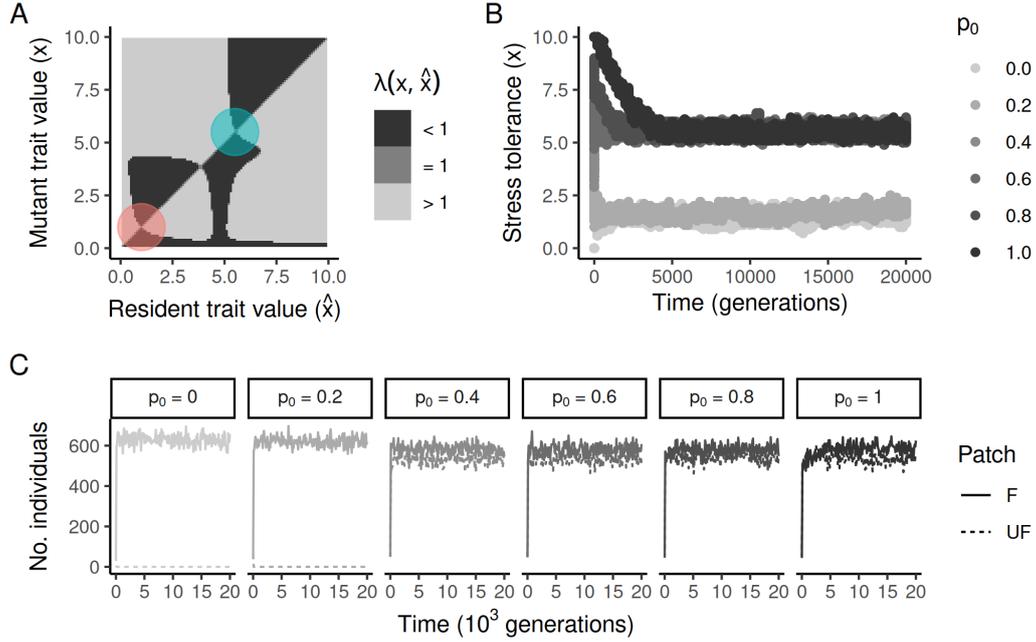
Figure 3: Model behavior in a single site ($n_{\mathrm{D}} = 1$) and under standard parameter values mimicking the conditions in a semi-arid landscape ($c = 0.5$, $K_{\mathrm{UF}} = 500$, $K_{\mathrm{F}} = 2\,000$, $\theta_{\mathrm{UF}} = 5$, $\theta_{\mathrm{F}} = 0$), pure selfing ($g = 0$) and a weak trade-off between stress tolerance and fecundity ($\epsilon = 0.1$). Other parameters are as per Table 1. (A) Pairwise invasibility plot (PIP) describing the expected adaptive dynamics of the model under these conditions (see Fig. S1 for how to interpret PIPs, and see Appendix for derivations). $\lambda(x, \hat{x})$ is the invasion fitness of mutant strategy x given resident strategy $\hat{x}$. Two alternative *continuously stable strategies* (CSS) are predicted: one stress-sensitive equilibrium strategy with stress tolerance too low to survive in the unfacilitated patches ($x \simeq 1 < \theta_{\mathrm{UF}}$, red circle), and one stress-tolerant equilibrium strategy with a high-enough tolerance to be able to survive in both patches ($x \simeq 5.5 > \theta_{\mathrm{UF}}$, blue circle). (B) Trait values of individuals through time in multiple simulations that vary in their initial stress tolerance (by way of the frequency p_0 of the tolerance alleles in the genome, see Fig. 1D). Depending on the starting conditions, one of the two equilibrium strategies predicted in A is reached. (C) Densities of individuals through time in both patches across the simulations shown in B. Populations reaching the stress-tolerant equilibrium strategy ($p_0 \geq 0.4$) are able to establish in both patches, while those reaching the stress-sensitive equilibrium strategy ($p_0 < 0.4$) are restricted to the facilitated patches.
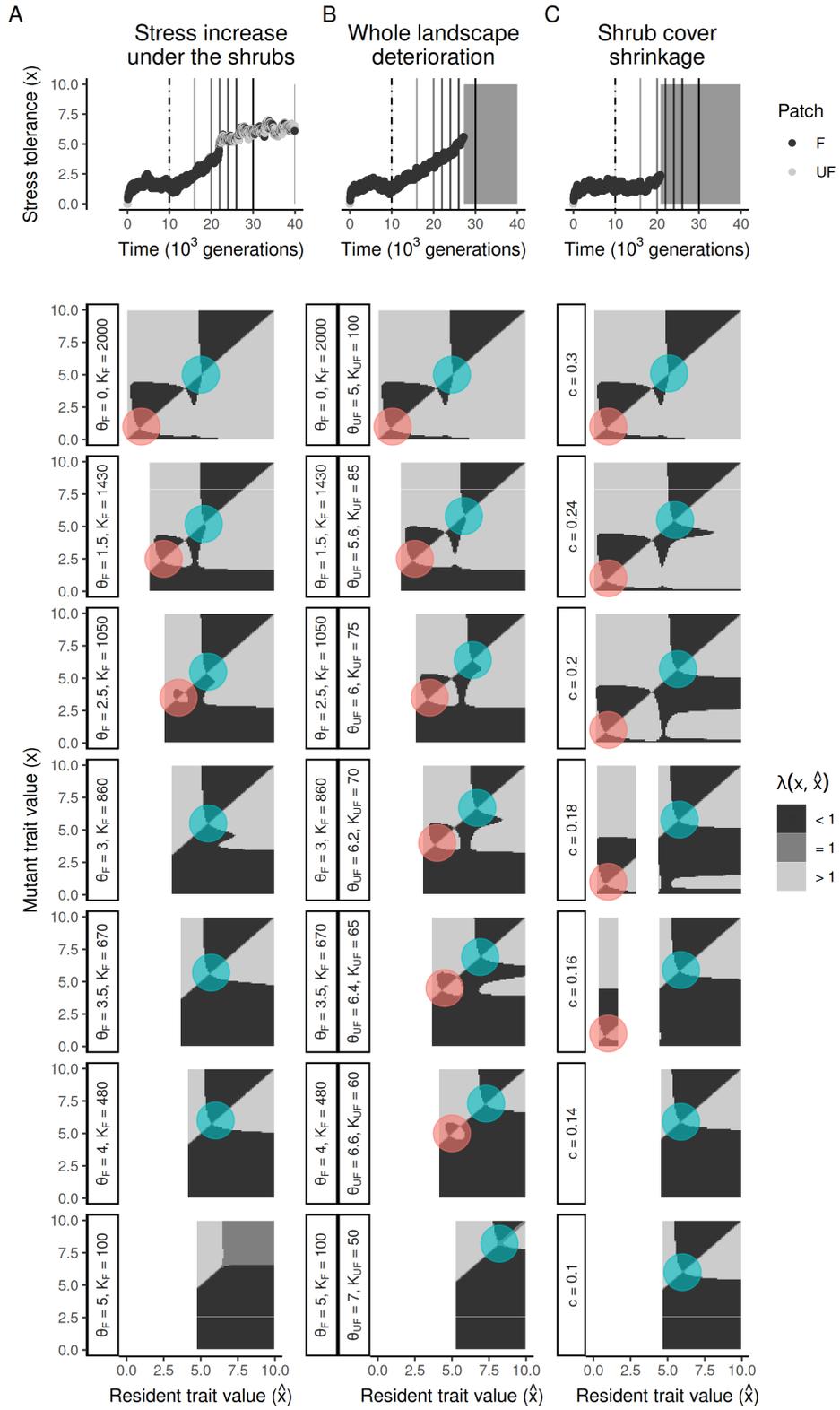
Figure 4: (See next page.)

Figure 4: Adaptive dynamics of the model during climate change. The top row shows three example simulations, each from one of our three climate change scenarios: (A) stress increase only under the shrubs, (B) whole-landscape deterioration, (C) shrinkage of the facilitated patches through time (these examples are taken from Fig. S9 with $\Delta t_{\mathrm{W}} = 20\,000$). Under each simulation, we show how the pairwise invasibility plot (PIP) changes through time, as environmental parameters change. Each PIP in a sequence (from top to bottom) is taken at one of the time steps shown with vertical bars in the corresponding simulation (top row). Red circles show the more stress-sensitive equilibrium. Blue circles show the more stress-resistant one (as in Fig. 3A).

Supplementary Results

S1 Branching points

Our Results show two possible alternative endpoints of evolution in the model (a sensitive and a tolerant strategy), in conditions resembling ecological facilitation in a harsh landscape. In some cases, however, these two strategies are not exclusive, and can both arise and coexist in the same environment. This happens when a population reaches an evolutionary branching point, i.e. an attractor of the evolutionary dynamics that becomes evolutionarily unstable, thus promoting the divergence of two strategies, once reached (see Fig. S1). It also requires a population to start off with a high stress tolerance, and the carrying capacity of unfacilitated patches to be sufficiently low (Fig. S16, see e.g. $K_{\mathrm{UF}} \leq 100$, while $K_{\mathrm{F}} = 2\,000$). In such cases, the population first evolves to the stress-tolerant equilibrium strategy predicted by its adaptive dynamics, then branches off into two distinct morphs: one that stays stress-tolerant, and one that evolves to become stress sensitive (Fig. S16). Frequency-dependent selection explains why this happens.

When the carrying capacity of unfacilitated patches is sufficiently high, the established tolerant strategy produces enough propagules across both habitats that no competing strategy (e.g. a stress-sensitive one with a higher reproductive output underneath the shrubs) can invade. The tolerant equilibrium strategy is then a stable endpoint of evolution, and not a branching point. However, as the carrying capacity of unfacilitated patches becomes sufficiently low (somewhere between $K_{\mathrm{UF}} = 100$ and 500 given the parameters tested here, see also Fig. S19), mutants investing slightly less in stress tolerance become a viable alternative, as they suffer less from the fecundity cost imposed by stress tolerance, and the propagule pressure from tolerant plants is no longer enough to prevent them from establishing under the shrubs. The result is two equivalent strategies coexisting in sympatry, in a so-called protected polymorphism where sensitive plants are found only underneath the shrubs and tolerant plants are found in both patches (Fig. S17D).

Note that while a stress-sensitive strategy can branch off from a stress-tolerant one, the reverse is not true. Even when the stress-tolerant strategy is a branching point, the stress-sensitive equilibrium strategy remains a stable attractor of the evolutionary dynamics that is not conducive to branching (Fig. S16A–B). The reason for this is the trade-off between survival and fecundity — the reproductive output of an established stress-sensitive strategy is higher than that of an established stress-tolerant one, such that an established sensitive strategy will not allow the rise of slightly more stress-tolerant mutants in the same way that a tolerant strategy would have left an opportunity for sensitive plants to invade and coexist. For these reasons, no branching occurs in our climate change experiment (see Results), where the population always starts as stress sensitive and not stress tolerant.

In general, we find that given the parameter values tested, facilitated patches should be able to host at least around 10 times as many plants as unfacilitated patches per unit area for the tolerant strategy to be a branching point (Fig. S18). We summarize in Figure S19 the kinds of evolutionary outcomes (in terms of branching points versus stable attractors) expected across

27

a wide portion of parameter space.

S2   Coexistence analysis

The coexistence of two morphs does not exclusively rely on in situ diversification of the two strategies from a single one (i.e. on branching points). Under some conditions, environmental parameters are such that sensitive and tolerant plants can stably coexist, even though they may not diversify in sympatry. This can happen, for example, in a metapopulation setting (with multiple demes, $n_D > 1$), where different strategies, evolved in relative geographical separation, come into secondary contact and are subsequently able to coexist within a site. Figure S20 illustrates this in a simulation where stress-tolerant and stress-sensitive plants are found in the same sites in a metapopulation with environmental parameters chosen such that divergence in sympatry is not possible.

Because coexistence does not rely exclusively on branching points, the scope for the maintenance of polymorphism is wider than for sympatric divergence only. By repeating our mutual invasibility analysis (see Methods) over thousands of parameter combinations, we find that indeed, many more parameter combinations allow for the stable coexistence of a sensitive and a tolerant morph, than would be expected solely based on branching points. This is particularly the case when the carrying capacity in the unfacilitated patches is too high to promote branching (e.g. $K_{UF} = 500$, Fig. S21). We confirmed the predictions of the mutual invasibility analyses by running simulations with two morphs in parts of parameter space where stable coexistence is predicted to occur, and those simulations remain dimorphic through time (Fig. S22). Altogether, these results suggest that migration among sites in a metapopulation is critical to the maintenance of local diversity in a facilitated system, as if diversity is lost locally, it may not be possible for one morph to re-evolve from the other in small mutational steps.

We also find that the maintenance of local diversity is sensitive to sexual reproduction and outcrossing. Indeed, the homogenizing effect of recombination on the gene pool usually breaks down branching points in the presence of gene flow (i.e. nonzero outcrossing, $g > 0$, Fig. S23). The coexistence of multiple morphs in the presence of gene flow may be rescued through mechanisms of assortative mating or some other sort of reproductive isolation, but we did not delve into these in the present study.

Supplementary Figures

A Continuously stable strategy

B Evolutionary repellor

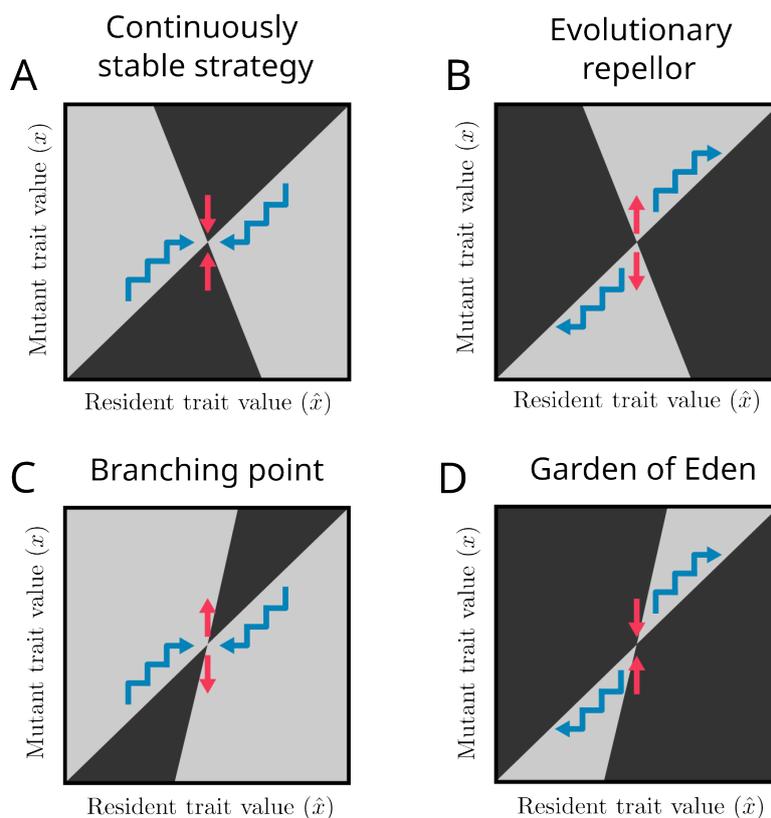**C** Branching point

D Garden of Eden

Figure S1: WA pairwise invasibility plot (PIP) is a phase plot showing, for each possible value of a trait fixed in a theoretical (monomorphic) *resident* population (here $\hat{x}$), the range of other values of the same trait that a rare *mutant* arising in a population of residents could have, and what the relative fitness of said mutant (here x) would be, compared to the resident. This relative *invasion fitness* determines whether a mutant can invade, and replace, a given resident. A PIP shows, in two different colors, all pairs of mutant and resident strategies where the mutant can invade (light gray here), and all pairs where the mutant cannot (dark gray). The graphical depiction predicts the dynamics of evolution through successive invasions (of mutants becoming the new residents, and so on, blue arrows). Eventually, a so-called *equilibrium* (or *singular*) strategy may be reached, where the direction of evolution changes (i.e. where the *isoclines* delimiting the invasion boundaries cross). Singularities that evolution by selection leads to (blue arrows) are *convergence stable*, but need not be endpoints of the evolutionary dynamics, as once reached they may be *evolutionarily stable* or not (red arrows).(A) Equilibrium strategies that are both convergence and evolutionarily stable are called continuously stable strategies (CSS) — they are stable endpoints of evolution.(B) Repellors are equilibria which are both convergence and evolutionarily unstable — selection leads away from them. (C) Branching points are convergence-stable attractors that are evolutionarily unstable once reached — they promote diversification into two morphs, each with their own trait value. (D) Gardens of Eden are repellors that would be evolutionarily stable if reached but in practice never are. For more information, see Geritz et al. (1998) and Otto and Day (2007).
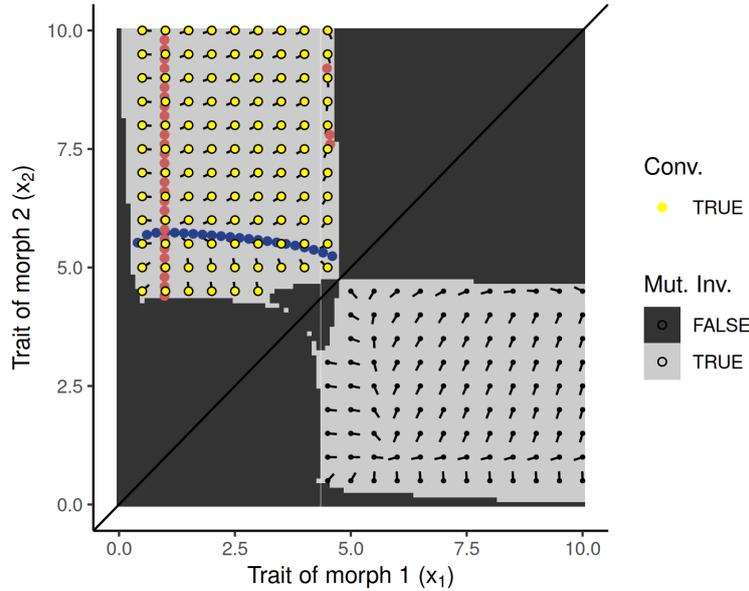
Figure S2: Mutual invasibility plot (MIP) and coexistence analysis. A MIP is a pairwise invasibility plot (PIP, see Figure S1) flipped over its own diagonal (Geritz et al., 1998). It can help understand the conditions under which two strategies can coexist in a population, and/or what happens *after* after a population has split into two groups, each with their own evolving trait (i.e. after a branching point has been reached, in the language of adaptive dynamics, see Appendix). The axes are no longer the mutant and resident strategies, as in a PIP, but the strategies (or traits) of two morphs present in the population. Light gray areas now indicate *mutual invasibility*, where both morphs can invade each other when one is taken as a mutant and the other as resident, and vice versa (the MIP is therefore symmetrical along its diagonal). Dark gray areas in the above figure are pairs of morphs that cannot coexist — one morph overtakes the other in those cases. That two morphs can mutually invade each other does not mean that they will remain in a stable coexistence, however, as evolution may lead to a point where they are no longer able to coexist. For this reason, in our analyses of MIPs we also plot a field of dimorphic *selection gradients* (tick marks), showing the direction in which selection is pushing both morphs to evolve (see Appendix for calculations). Potential endpoints of dimorphic evolution are points in the MIP where selection no longer pushes in any direction. In our study, we graphically find those points by generating null isoclines, i.e. lines in the MIP where the selection gradient is zero in one of its two dimensions (red and blue dots). The crossing points between isoclines are *equilibrium coalitions* of mutually invasible morphs, that is, pairs of strategies that can coexist and will not evolve more once reached. However, similar to the convergence stability problem of PIPs, here we need to know, for a given equilibrium coalition, whether evolution pushes towards or away from it. We determine this by evaluating, for each dimorphic selection gradient (i.e. tick mark) that was computed in the area of mutual invasibility (i.e. the gray zone), the proportion of those gradients pointing towards said equilibrium. The coalitions expected to converge towards the equilibrium coalition (at the crossing of the red and blue isoclines), are labeled in yellow in the plot. The proportion of all tick marks pointing towards a given equilibrium is termed the *basin of attraction* of that equilibrium, and is used as a proxy for the propensity of the system to reach stable coexistence of two morphs in the long term. The example MIP shown here is that of Figure S17B.
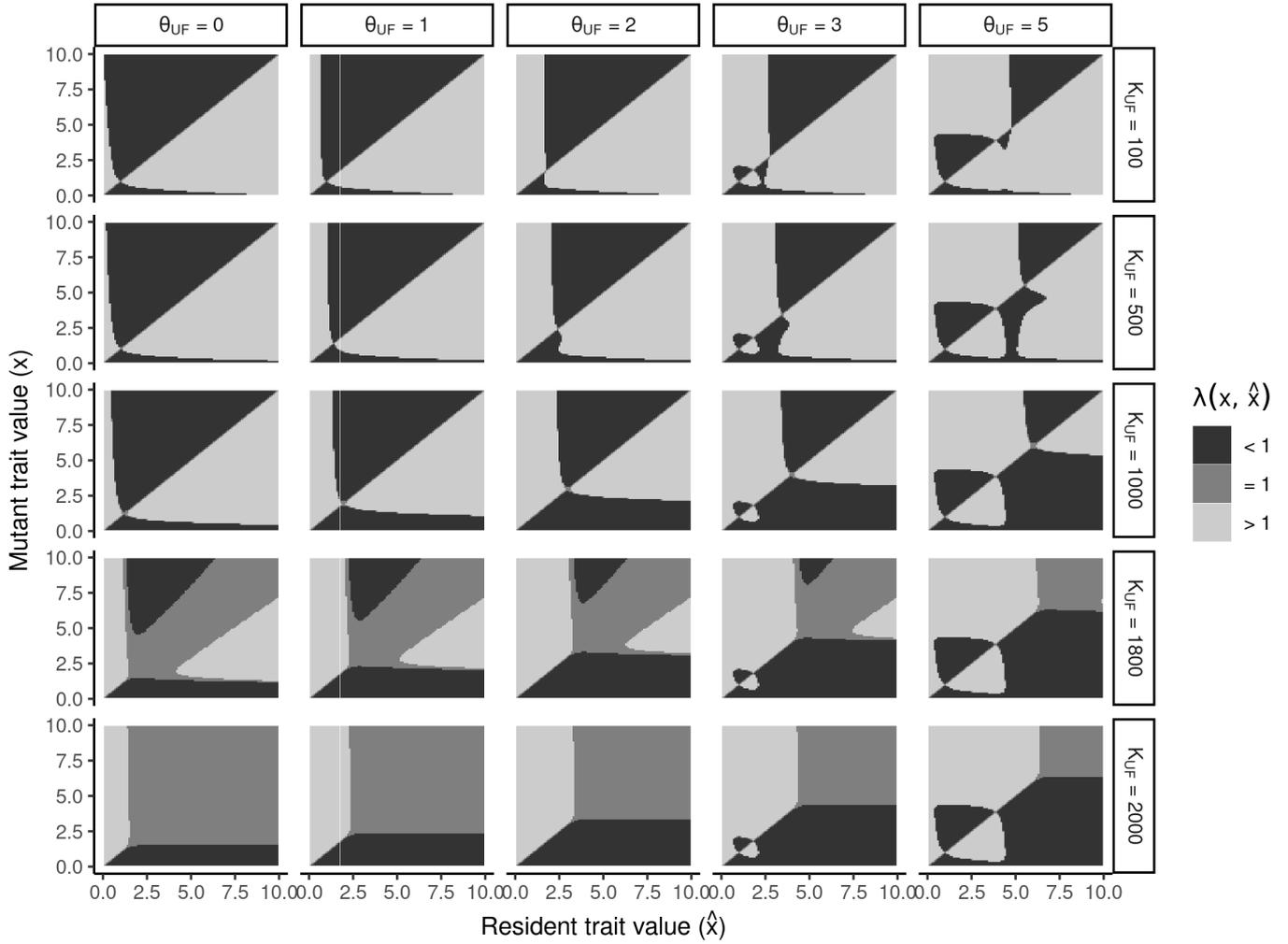
Figure S3: Effects of the level of stress θ_{UF} and carrying capacity K_{UF} of the unfacilitated patches, on the adaptive dynamics of the model. Other parameter values are the same as in Fig. 3. Note: in zones where $\lambda(x, \hat{x}) = 1$, mutant and resident have the same fitness.
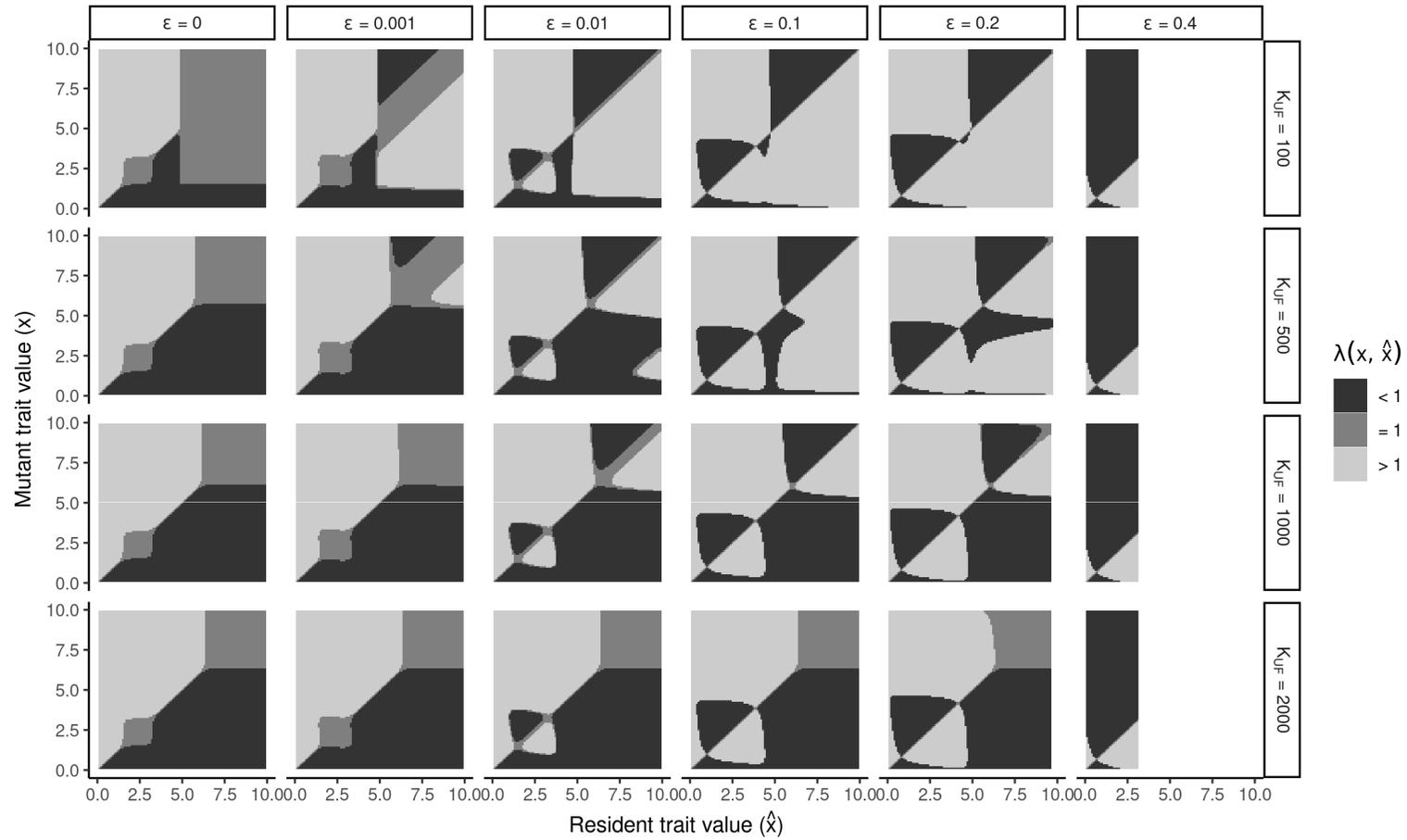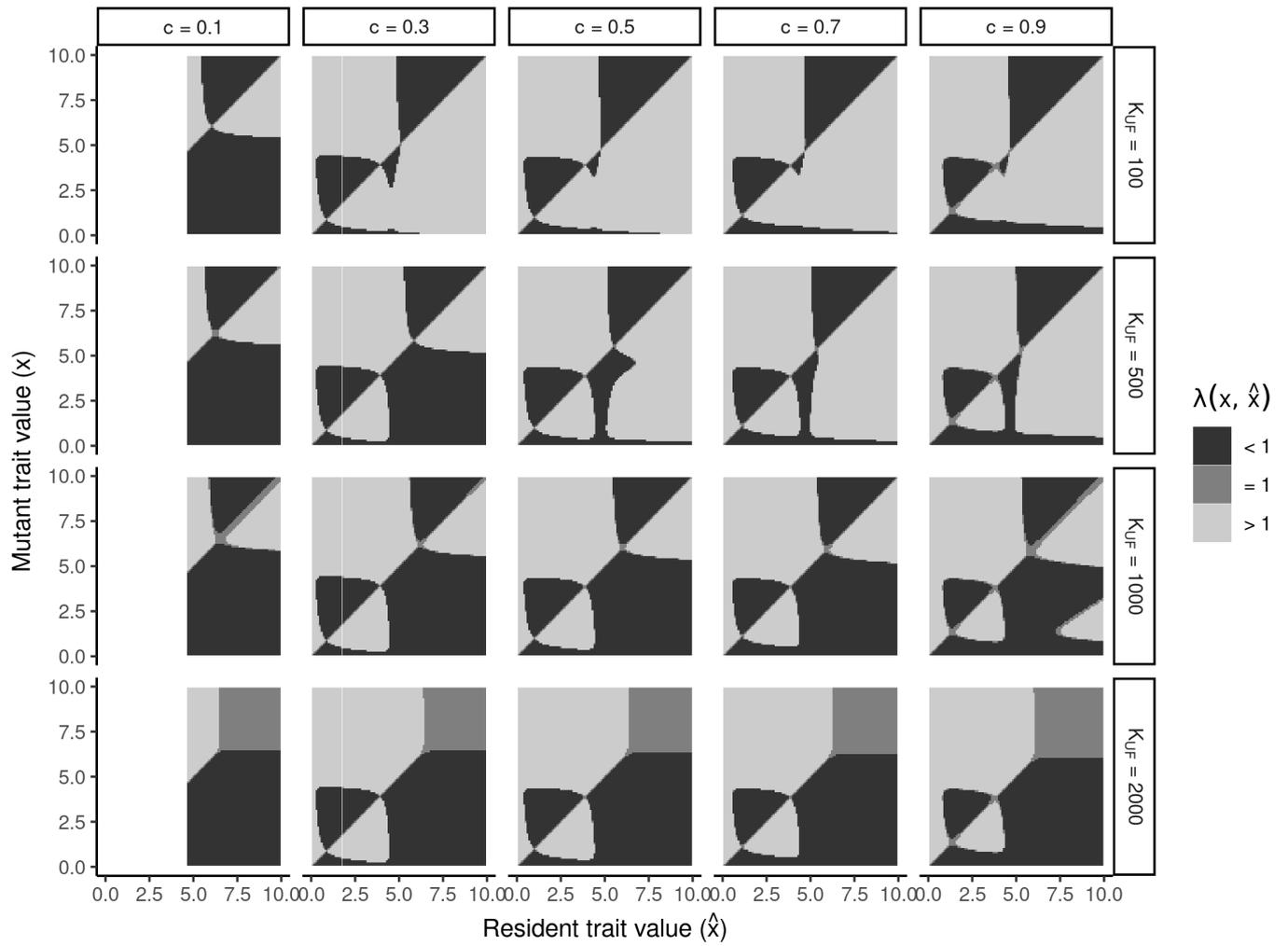
Figure S4: Effects of trade-off strength ϵ and carrying capacity K_{UF} of the unfacilitated patches, on the adaptive dynamics of the model. Other parameters are as per Fig. 3. Note that blank regions of the plot mean that no viable resident population can be sustained for these trait values.

Figure S5: Effects of shrub cover c and carrying capacity K_{UF} of the unfacilitated patches, on the adaptive dynamics of the model. Other parameters are as per Fig. 3.
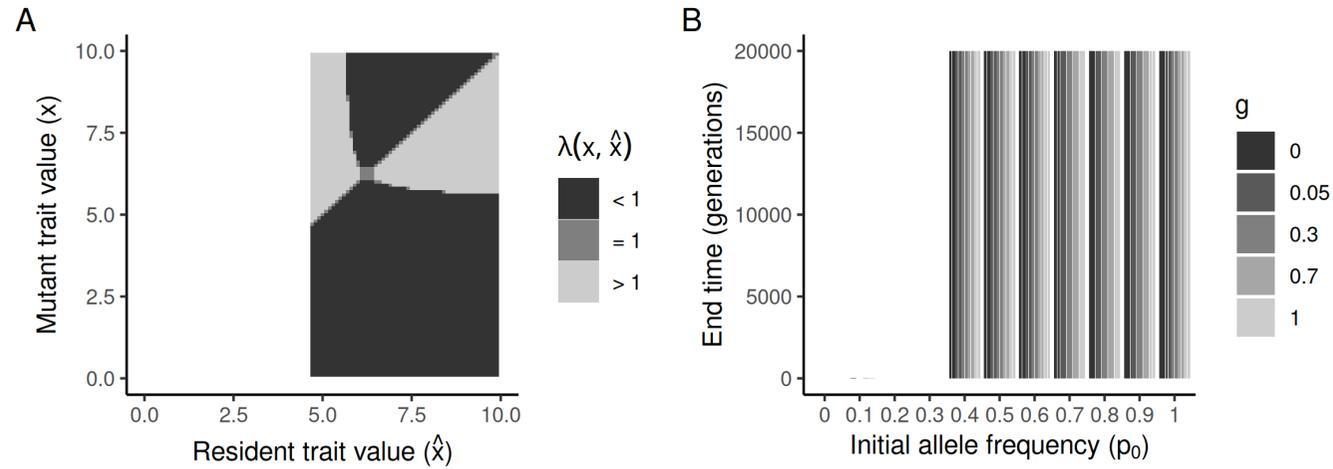
Figure S6: Population extinction in an inhospitable landscape with low shrub cover ($c = 0.1$, other parameters as per Fig. 3). (A) Predicted adaptive dynamics under these conditions. The shrub cover is too low for a stress-sensitive strategy to be viable. (B) Simulations are run under different rates of outcrossing g. Only simulations (bars) with a population starting off with a sufficiently high level of stress tolerance ($p_0 \geq 0.4$) can survive all the way to the end of the simulation time. The ones starting with a too low frequency p_0 of tolerance alleles in their genome go extinct almost immediately.
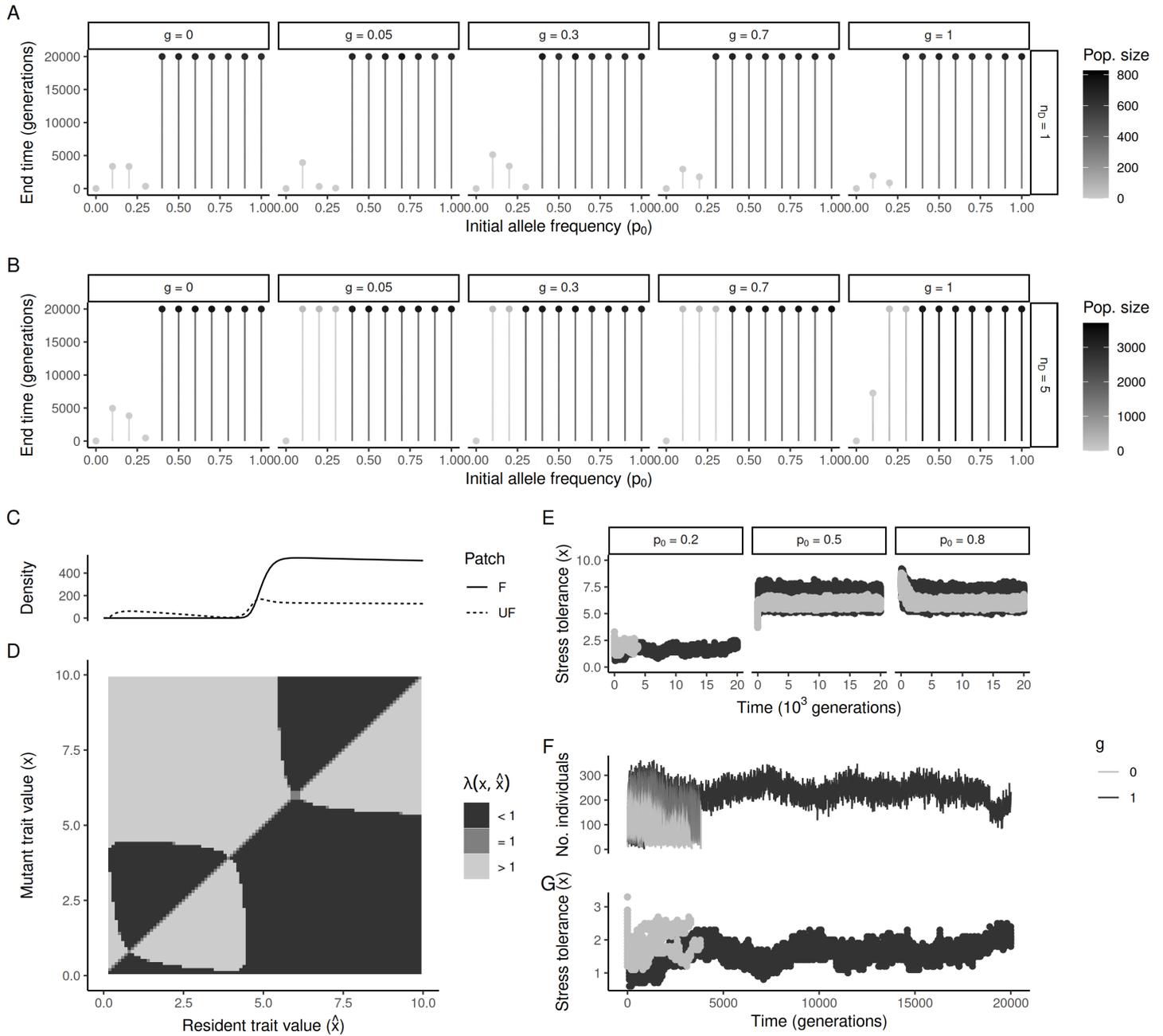
Figure S7: (See next page.)

Figure S7: Outcrossing can protect low-density stress-sensitive populations from stochastic extinction. (A) Simulations run in an environment with one deme ($n_D = 1$), low shrub cover ($c = 0.2$) and across different rates of outcrossing g (as per Fig. S6B). Similar to $c = 0.1$ (Fig. S6), stress-sensitive populations rapidly go extinct. (B) With more demes ($n_D = 5$), nonzero levels of outcrossing ($g > 0$) help maintain initially sensitive populations at low densities. Studying the adaptive dynamics of the model reveals why. (C) The predicted equilibrium density of stress sensitive strategies in one deme is above zero in such environments, meaning that they could in theory survive, but at much lower densities than stress tolerant plants. (D) Indeed, the stress sensitive strategy is a reachable, stable evolutionary attractor of the adaptive dynamics under these conditions. (E) Comparison of simulations with $g = 0$ (pure selfing) and $g = 1$ (pure outcrossing) across three different starting points taken from B. Besides displaying generally higher phenotypic variation than selfing populations, outcrossed populations typically reach the same evolutionary endpoints, but avoid extinction even when they remain stress-sensitive ($p_0 = 0.2$). (F–G) Zooming in on the leftmost panel in E ($p_0 = 0.2$) and looking at densities (F) and trait evolution (G) reveals that the selfing population ($g = 0$) oscillates more in trait value, probably due to drift. This suggests that outcrossing, by increasing the genetic variance, keeps the population close to its evolutionary equilibrium and prevents it from drifting towards trait values for which the population density that can be sustained is dangerously close to zero (and stochastic demographic fluctuations can easily push the population over that edge).
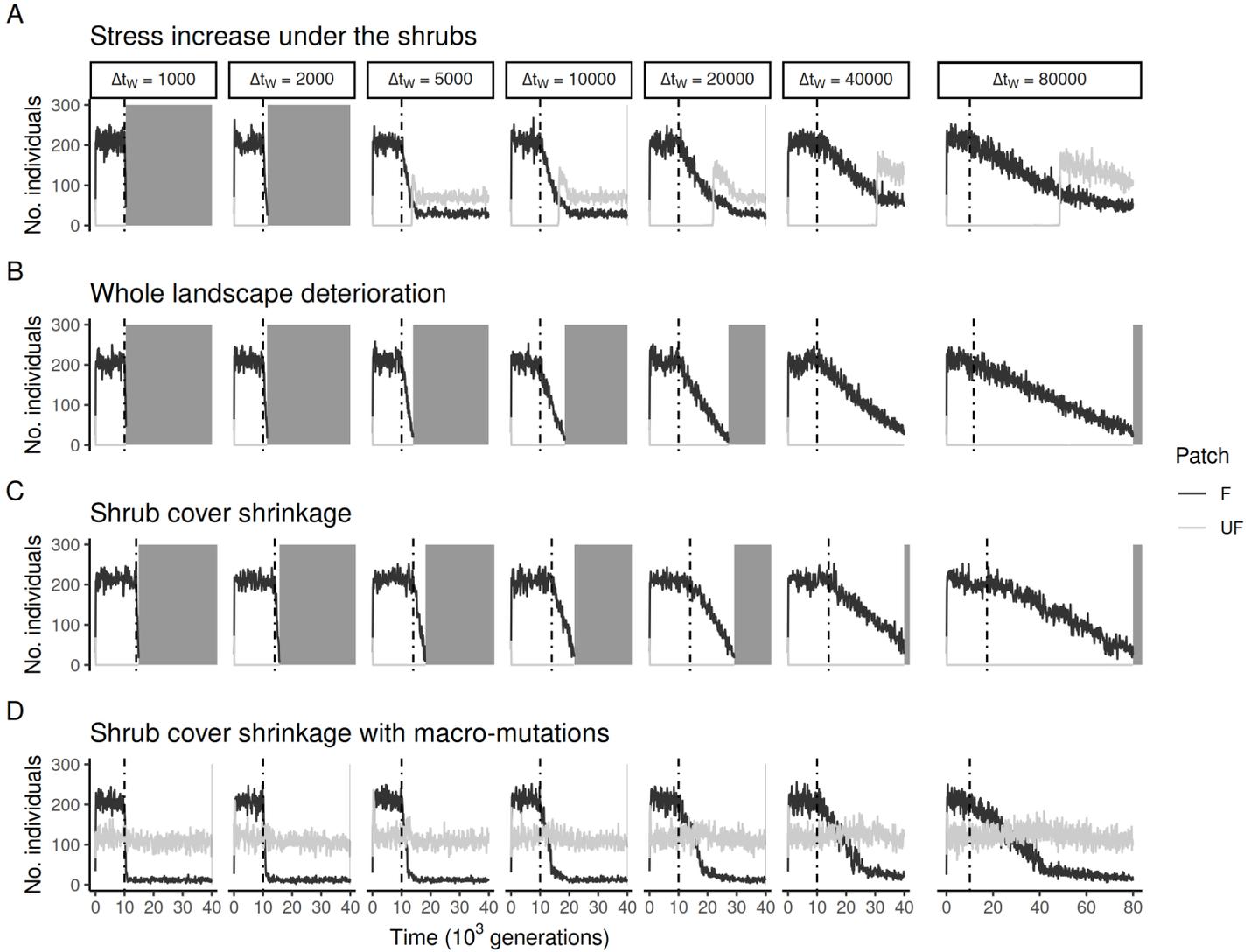
Figure S8: Densities through time across the three scenarios of our climate change experiment (see Methods and Table 2): (A) stress increase only under the shrubs (parameters θ_F and K_F change from 0 to 5 and from 2 000 to 100, respectively); (B) whole-landscape deterioration (θ_F changes from 0 to 5, K_F from 2 000 to 100, θ_{UF} from 5 to 7, and K_{UF} from 100 to 50); and (C) shrinkage of the facilitated patches through time (parameter c changes from 0.3 to 0.1). All other parameters are as per Fig. 2. An extra scenario (D) revisits the shrub-cover shrinkage scenario (C), but with macromutations scattered throughout the genome and allowing large mutational steps during phenotypic evolution (in each simulation 10 loci were sampled at random and their effect size was increased from $\eta = 0.1$ to $\eta = 5$, see Table 1). For each scenario, different durations of environmental change Δt_W are tested. Gray rectangles in the background mean that the population went extinct.
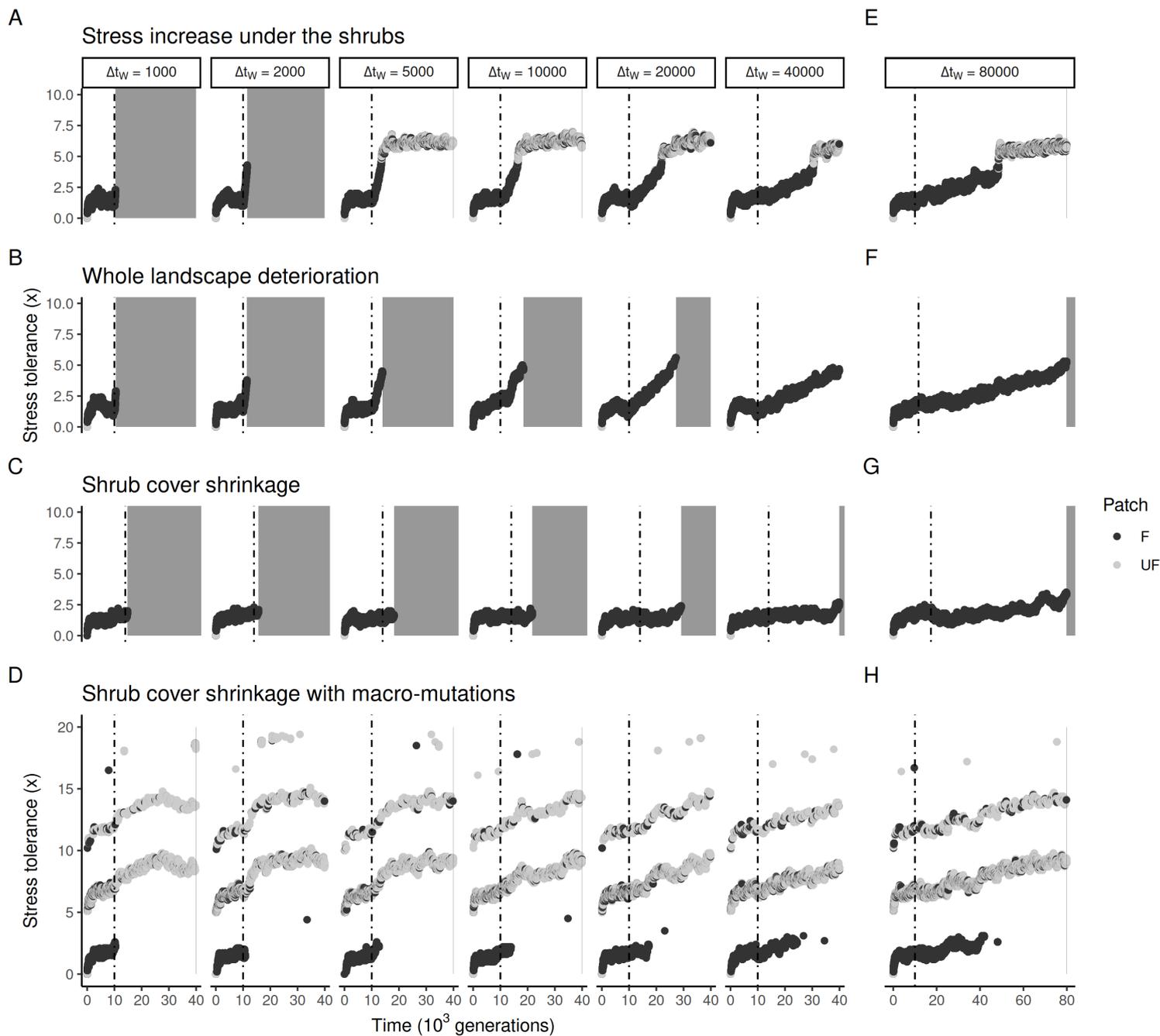
Figure S9: Stress tolerance evolution in our climate change experiment. Each point represents an individual. The simulations are the same as in Figure S8. Note that although scenarios B and C both almost invariably lead to extinction, in the case of the whole-landscape deterioration scenario (B), the population evolves its stress tolerance as the environment changes, while it remains more-or-less constant in the shrub-cover shrinkage scenario (C).
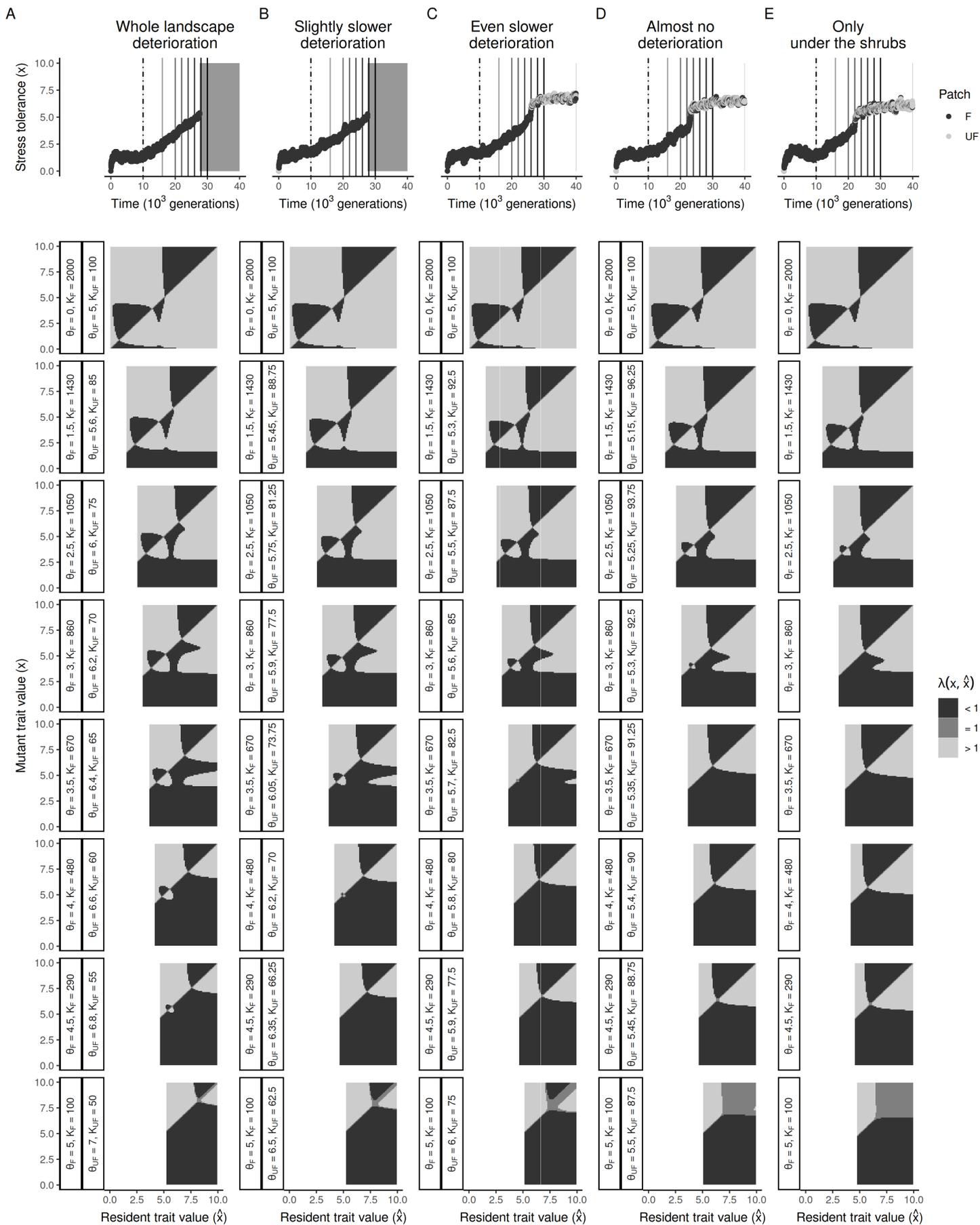
Figure S10: (See next page.)

39

Figure S10: Adaptive dynamics across paces of landscape deterioration. Legend is as per Fig. 4, except here, the investigate scenarios span a range of rates of deterioration (i.e. increase in stress θ and decrease in carrying capacity K) of the unfacilitated patches relative to the facilitated patches. In all cases, θ_F goes from 0 to 5, and K_F goes from 2 000 to 100 throughout the $\Delta t_W = 20\,000$ time steps of climate change. However, the magnitude of change of the unfacilitated patches over that time varies, starting from from $\theta_{UF} = 5$ and $K_{UF} = 100$, to (A) $\theta_{UF} = 7$ and $K_{UF} = 50$ (the whole-landscape deterioration scenario shown in Fig. 4B), (B) $\theta_{UF} = 6.5$ and $K_{UF} = 87.5$, (C) $\theta_{UF} = 6$ and $K_{UF} = 75$, (D) $\theta_{UF} = 5.5$ and $K_{UF} = 62.5$, or (E) remaining the same throughout (which is the scenario with stress increase only under the shrubs in Fig. 4A).
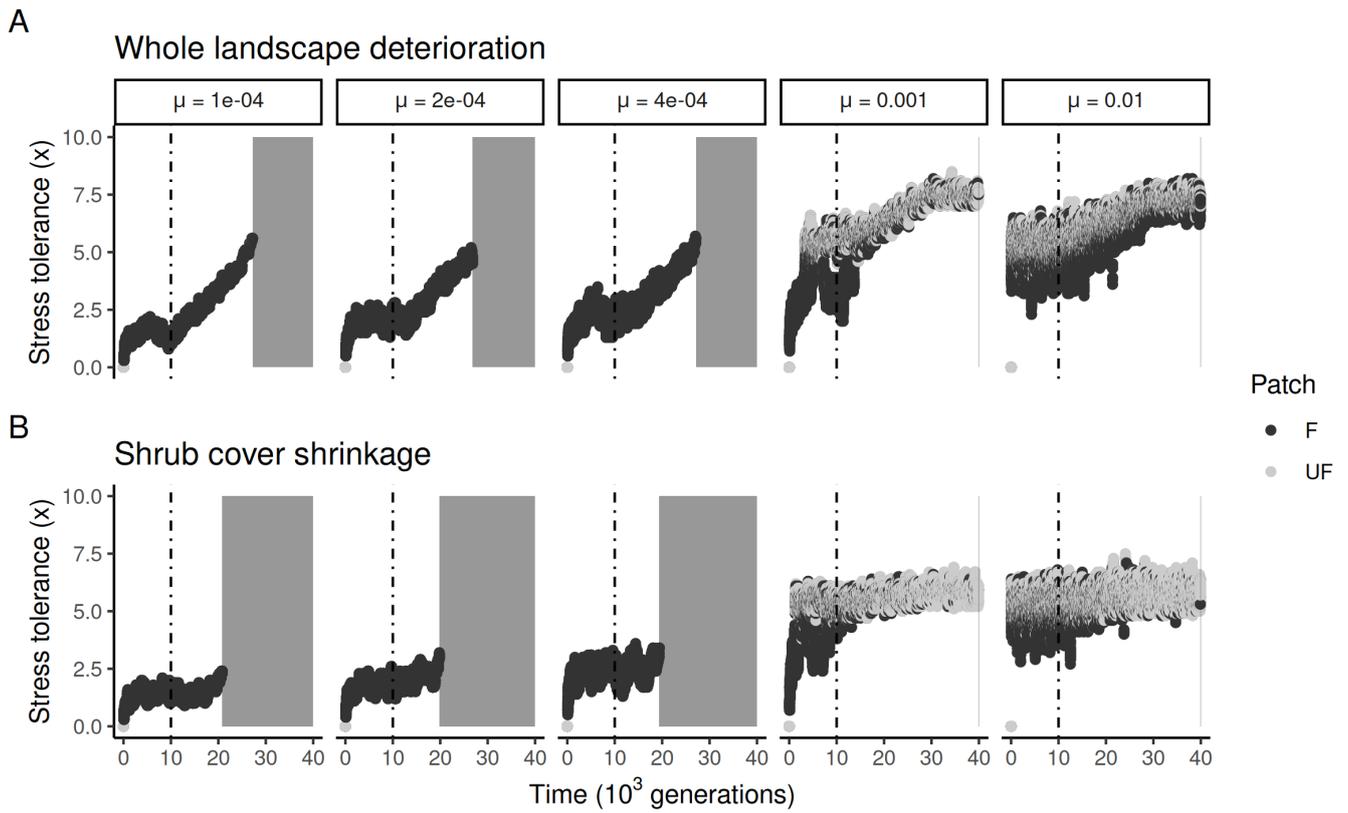
Figure S11: Stress tolerance evolution in climate change simulations across mutation rates μ, in (A) the whole-landscape deterioration scenario, and (B) the shrub-cover shrinkage scenario. Parameters are otherwise the same as in Fig. 4 ($\Delta t_W = 20\,000$).
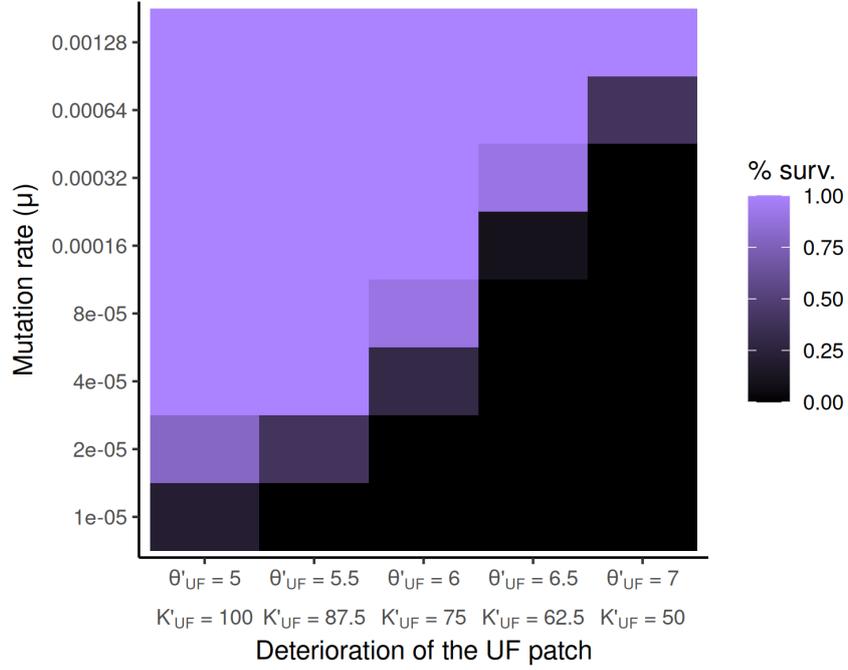
Figure S12: Population rescue across mutation rates μ and rates of deterioration of the unfacilitated patches (i.e. final values θ'_{UF} and K'_{UF} of environmental stress and carrying capacity, respectively, after $\Delta t_{\text{W}} = 20\,000$ time steps of climate change). Parameters are otherwise the same as in Fig. S10. For each combination of parameters, we ran 10 replicate simulations and measured the proportion that survived extinction. Note the non-linear scale of the mutation rate axis.
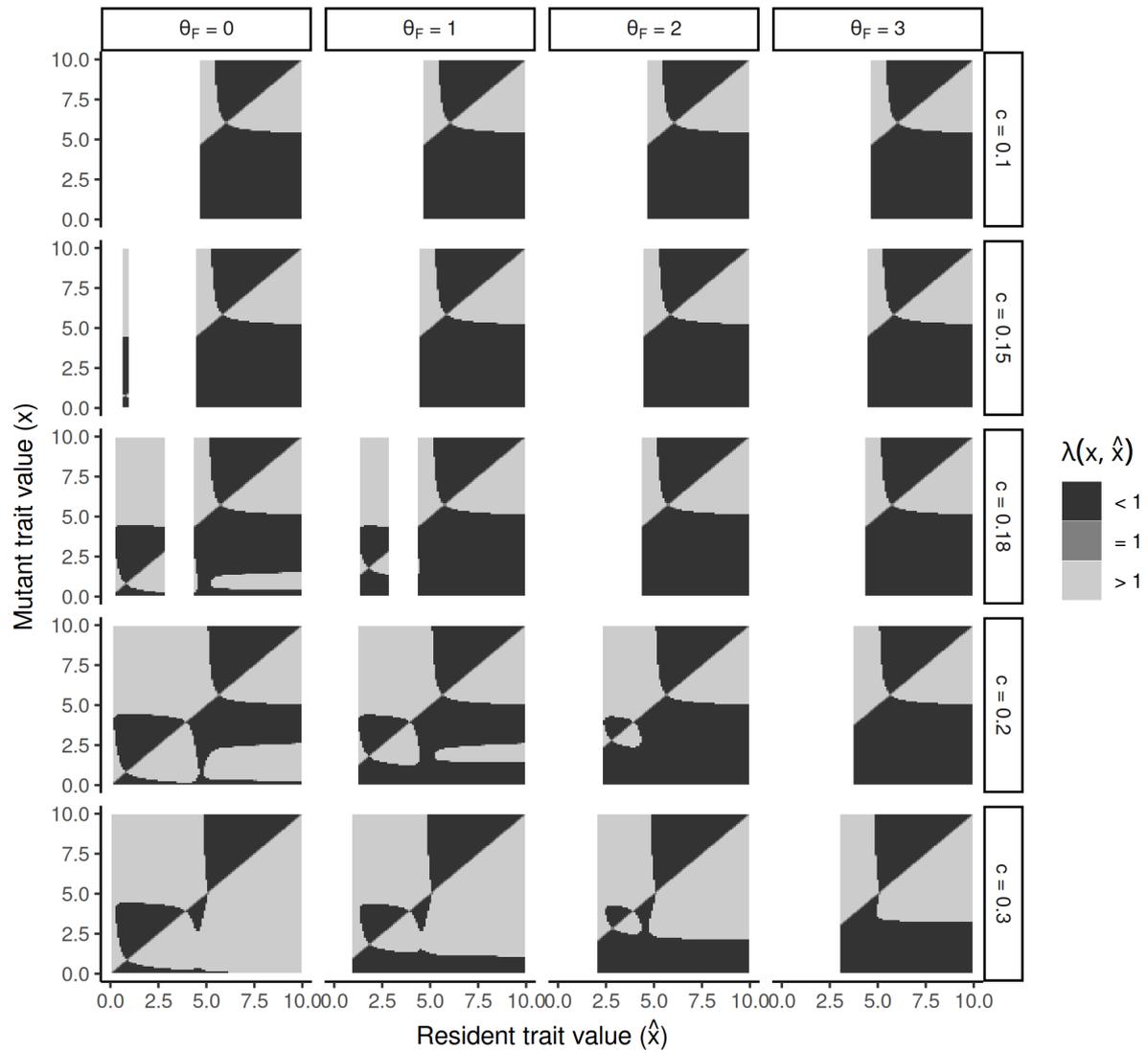
Figure S13: Effects of stress level θ_F and cover c in the facilitated patches on the adaptive dynamics of the model. Parameters otherwise as per Fig. 3.
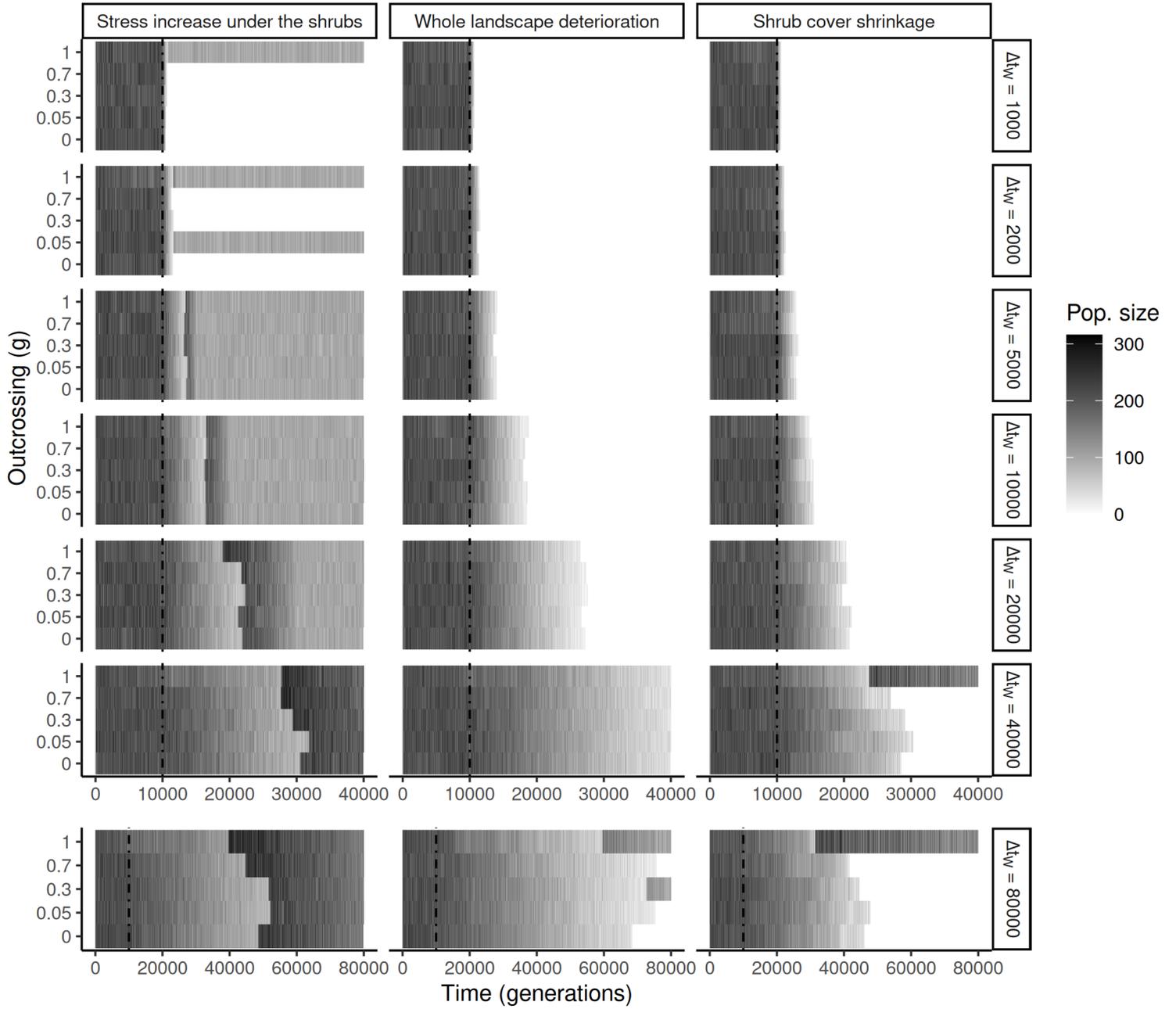
Figure S14: Evolutionary rescue under climate change with outcrossing. Each panel shows the total number of individuals through time in simulations run as per Fig. S8 (same parameters), but with varying rates of outcrossing g, the probability that a seed is fertilized by a pollen grain (see Methods). Simulations with $g = 0$ (pure selfing) are those shown in Fig. S8. Vertical dashed lines show the time at which climate starts to change, and blank tiles mean that the population went extinct. Note the difference in time scale between the last row and the rest.
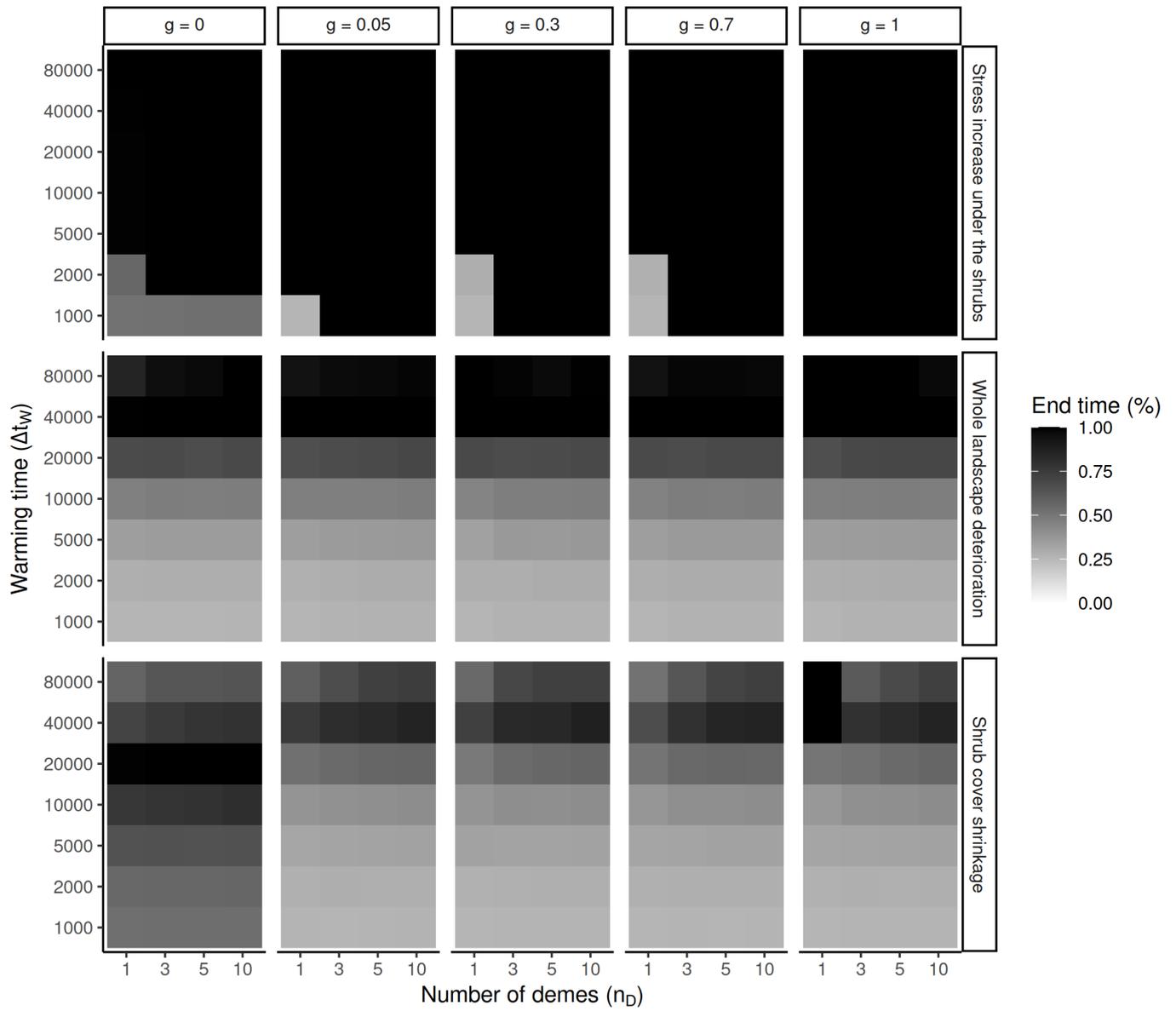
Figure S15: Effect of metapopulation size on evolutionary rescue. The simulations are essentially the same as in Figure S14, but have been extended to different numbers of demes n_D. Here, end time refers to the proportion of the total allocated time reached by the population (a value of 1 meaning that the population survived all the way to the end).
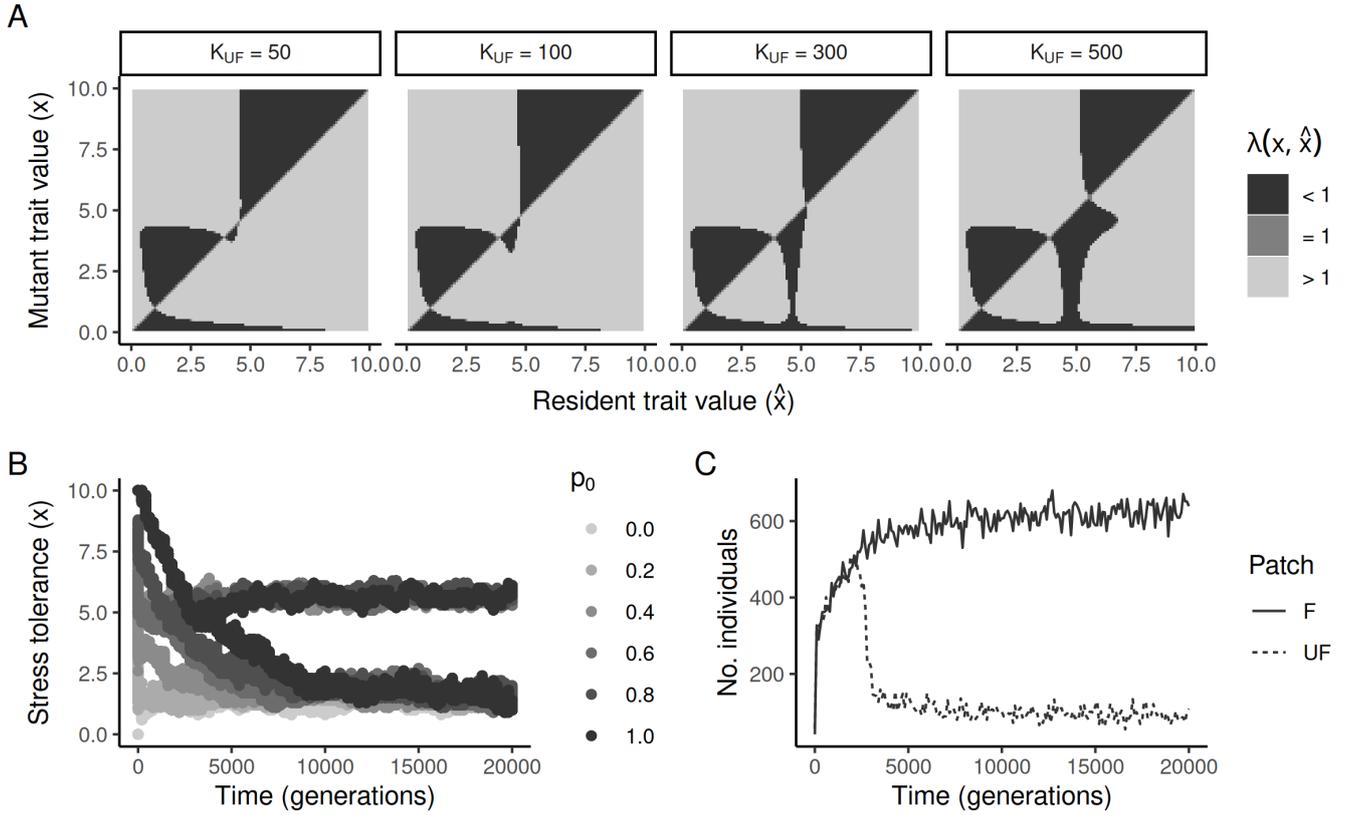
Figure S16: Branching of two stress tolerance strategies in sympatry. Under certain conditions (e.g. unfacilitated patches being particularly inhospitable and having a low carrying capacity K_{UF}), a population starting off with a high stress tolerance can split into two groups of individuals — one group maintaining a stress-tolerant strategy and the other evolving a stress-sensitive strategy. (A) Predicted adaptive dynamics across values of the carrying capacity K_{UF} (all other parameters being as in Fig. 3). Out of the two evolutionary equilibria identified in Fig. 3A, the top one, which is a convergence- and evolutionarily stable strategy (i.e. a continuously stable strategy, CSS) when K_{UF} is high, turns into a *branching point* (a convergence-stable but evolutionarily unstable strategy) as K_{UF} goes down ($K_{UF} \leq 100$). (B) Stochastic simulations with $K_{UF} = 100$ and different starting trait values. The predicted branching occurs in populations starting with a high stress tolerance as they reach the branching point, but not in populations starting with a low stress tolerance ($p_0 < 0.4$), which instead reach the lower, solely stress-sensitive CSS (near $x \simeq 1$). (C) Densities of individuals in the simulation in B with $p_0 = 1$, showing a shift in patch occupancy as a stress-sensitive strategy branches off from the stress-tolerant one.
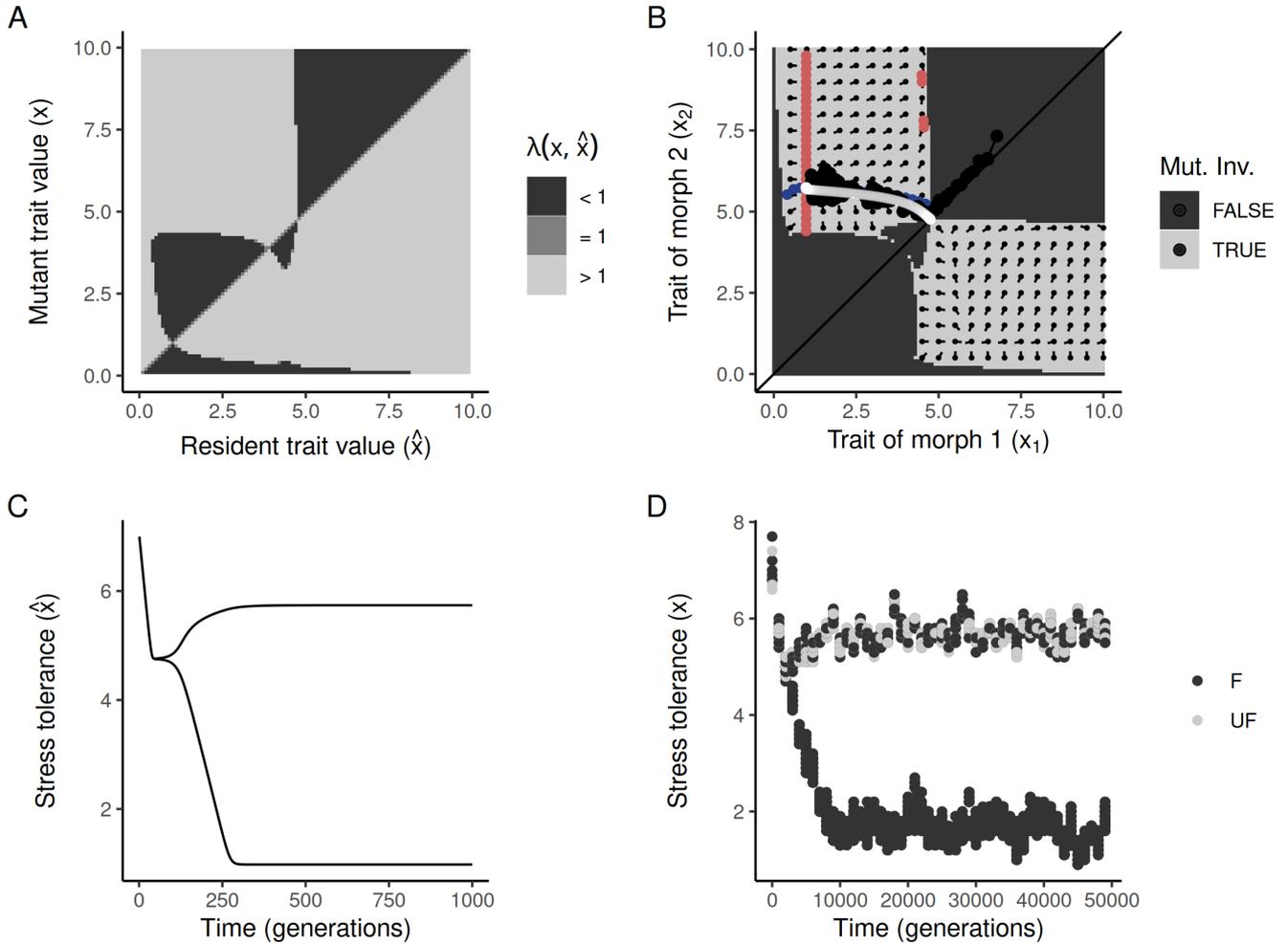
46

Figure S17: Details of what happens at a branching point in the model. (A) Predicted adaptive dynamics in the case of Figure S16A where $K_{UF} = 100$. Under these conditions, the PIP shows a continuously stable strategy (bottom equilibrium strategy near $x \simeq 1$) and a branching point (top equilibrium near $x \simeq 5$), separated by a repellor (see Fig. S1 for the kinds of equilibria possible in adaptive dynamics). (B) By flipping the PIP over its diagonal, we get a mutual invasibility plot (MIP), which shows the predicted adaptive dynamics of the model after the branching point has been reached, with dimorphic fitness isoclines showing in red and blue (see Fig. S2 for details). On top of that, we overlay the trajectories of one particular stochastic simulation (black points) and one particular deterministic simulation (white line), both showing agreement with the predicted adaptive dynamics. (C) Deterministic simulation of evolutionary branching shown in B (see Appendix). (D) Stochastic simulation shown in B. Both simulations are run under the same parameters as panels A and B, albeit with extra parameters $\mu_x = 0.01$ and $\sigma_x = 0.5$ proper to the deterministic simulation model, and $p_0 = 0.7$ and $g = 0$ proper to the stochastic simulation model (Table 1).
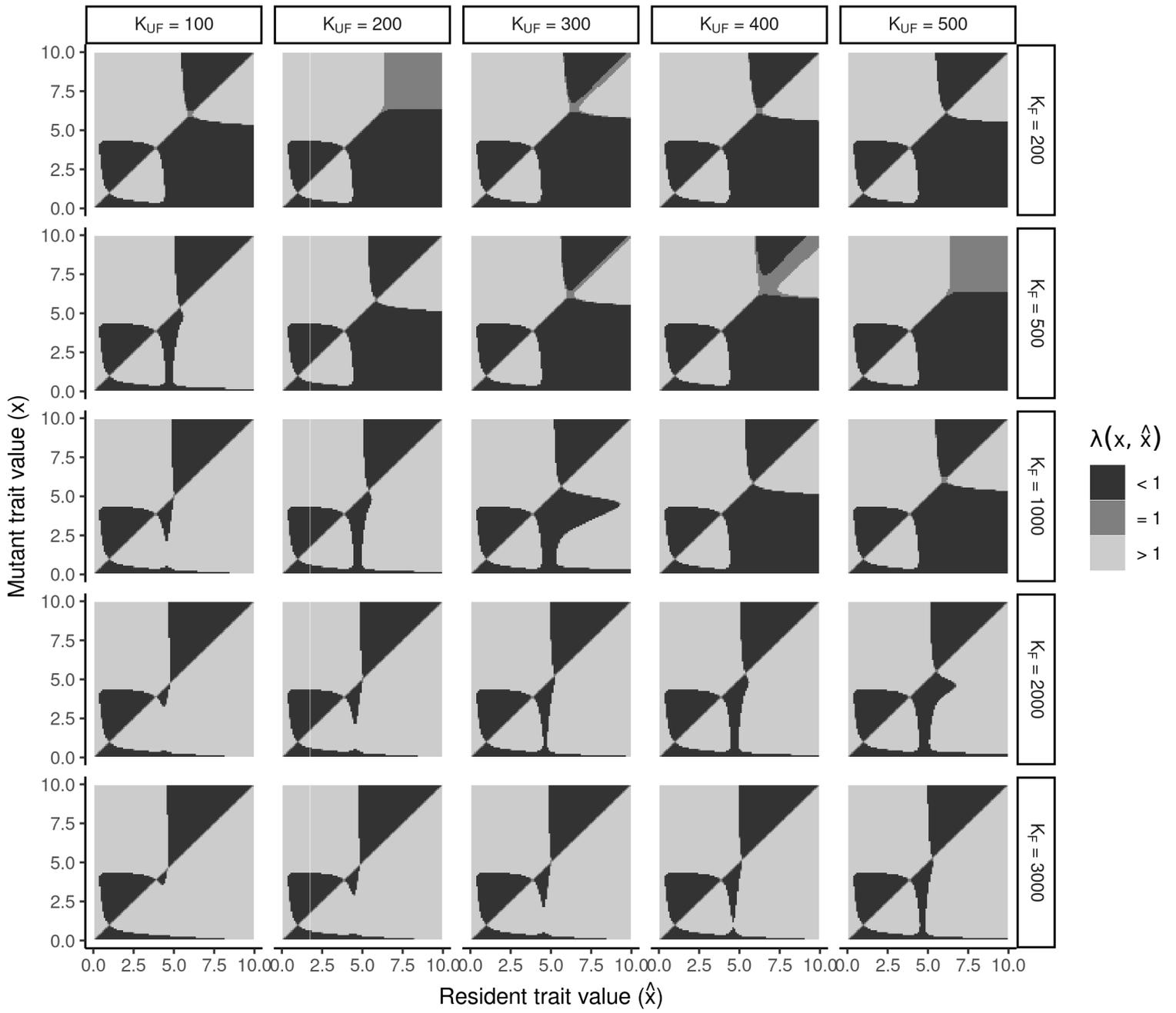
Figure S18: Effects of carrying capacity of the unfacilitated patches K_{UF}, and of the facilitated patches K_{F}, on the adaptive dynamics of the model. Other parameters are as per Fig. 3.
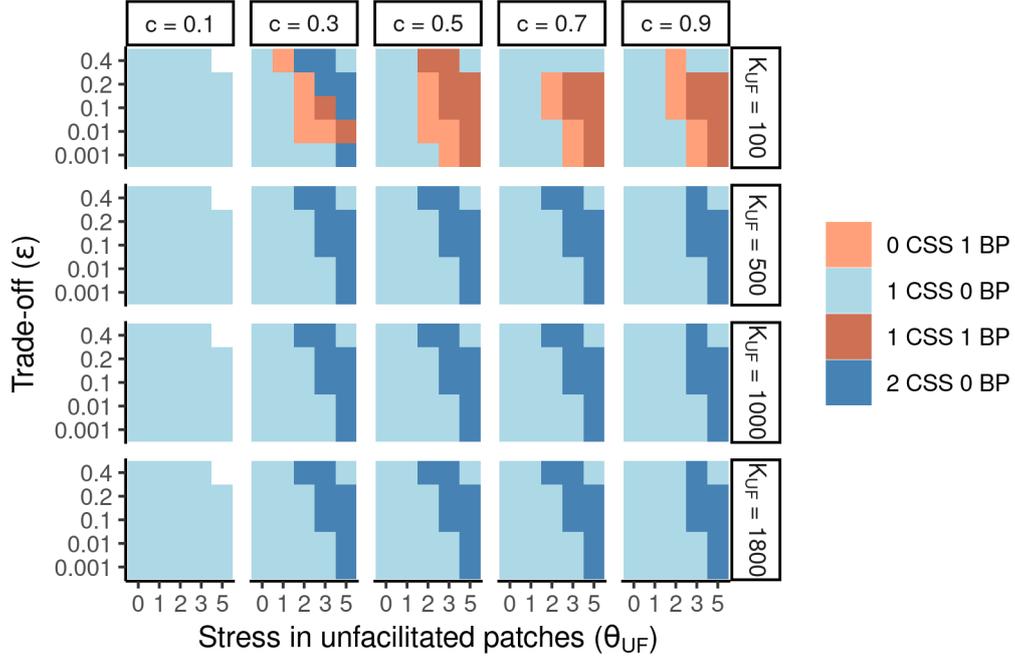
Figure S19: Types of evolutionary equilibria found across parameter space. For each combination of parameters, we used derivations of the invasion fitness function (see Appendix) to compute selection gradients and criteria for evolutionary and convergence stability, which we used to search for evolutionary singularities and evaluate their types (see Fig. S1). In our exploration, we find various combinations of continuously stable strategies (CSS) and branching points (BP) (repellors are not mentioned). Blank tiles indicate that no equilibrium is found. Parameters not mentioned in this figure are as per Fig. 3.
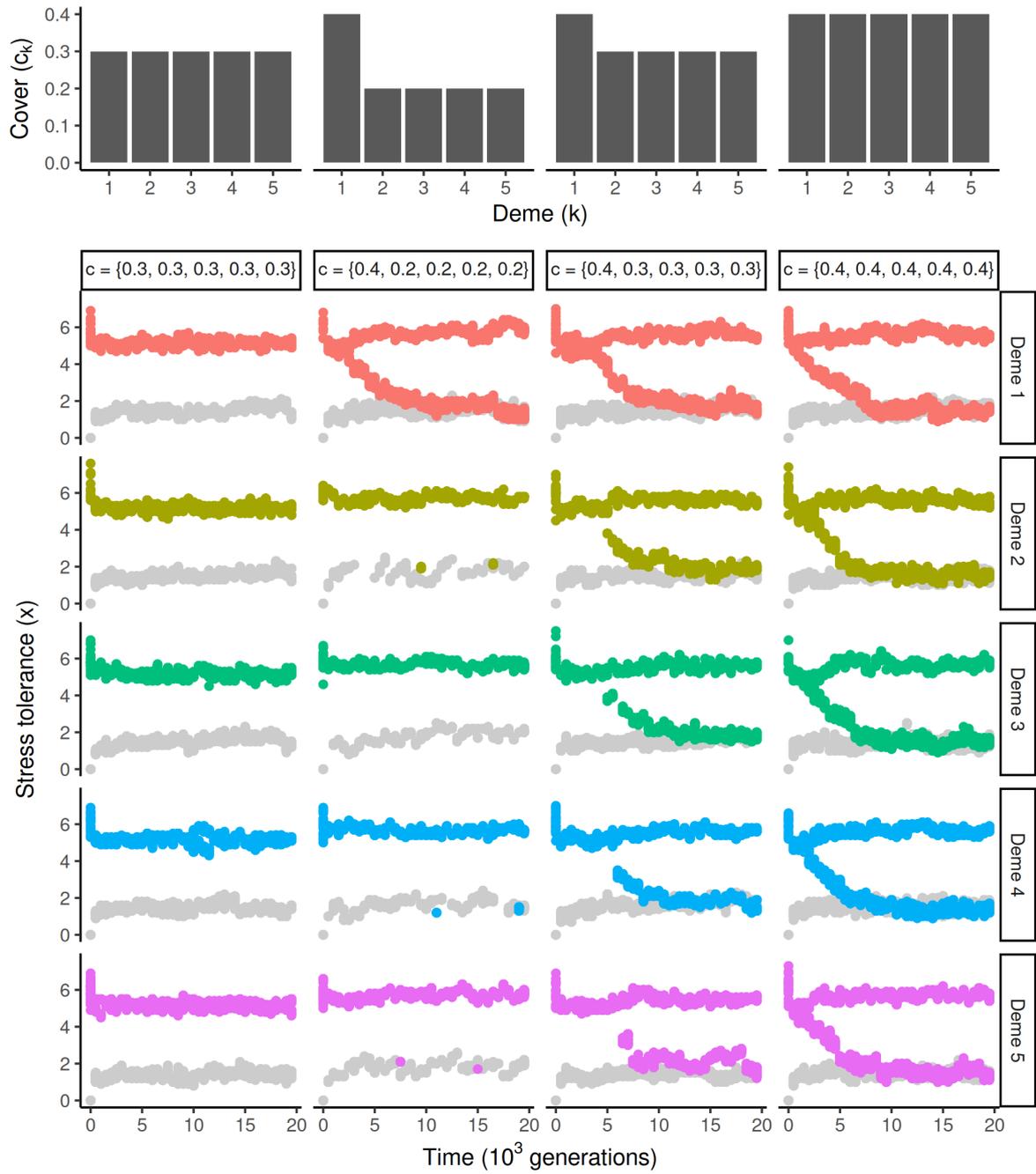
Figure S20: (See next page.)

Figure S20: Coexistence of morphs through secondary contact. In some cases, the stress-tolerant and stress-sensitive strategies can coexist within a deme without having diversified in sympatry (i.e. without the need for a branching point, and as predicted in Fig. S21). To show this, we ran a simulation experiment with five demes ($n_D = 5$), in which two morphs could originate in sympatry in the first deme, but required migration to establish in the other demes. We did so by tuning the shrub cover c of the different demes (top panel), as we established that a low shrub cover ($c = 0.2$) prevents the establishment of a stress-sensitive strategy, an intermediate shrub cover ($c = 0.3$) allows the stress-sensitive strategy to be viable, and a higher shrub cover ($c = 0.4$) turns the stress-tolerant equilibrium strategy into a branching point (all other parameters being the same as in Fig. 3 except $K_{UF} = 100$, see also Fig. S19). We then tested different combinations of shrub covers across the five demes, always starting with a population with an already high stress tolerance (allele frequency $p_0 = 0.6$). The first scenario (column 1) serves as a negative control, where shrub cover ($c = 0.3$ in all demes) could in theory support stress-sensitive plants, but that equilibrium is not reached because the two equilibrium strategies are exclusive alternative endpoints of the adaptive dynamics, and the stress-tolerant equilibrium is reached instead (e.g. as in Fig. 3). For comparison, we ran simulations under the same conditions but starting with low stress tolerance ($p_0 = 0$, gray points in the background) to show that the stress-sensitive equilibrium is reached instead in that case. The second scenario (column 2) allows branching in the first deme ($c = 0.4$) but the stress-sensitive strategy is not viable in the other demes ($c = 0.2$). Hence, we see occasional stress-sensitive migrants appearing in those demes, but never establishing a coexistence with the stress-tolerant plants. Note that in the low-tolerance version of that scenario (gray points) demes 2 to 5 seem more scarcely populated than in other simulations, confirming that they are mostly maintained through migration from deme 1. The third scenario (column 3) allows branching only in the first deme ($c = 0.4$) but allows coexistence of the two morphs in the other demes ($c = 0.3$). After a lag of a few thousand generations, the stress-sensitive strategy eventually colonizes all demes, and both strategies end up coexisting through secondary contact. The last scenario (column 4) serves as a positive control, as shrub cover is high enough ($c = 0.4$) to promote branching in all demes. In that case, the stress-sensitive strategy evolves from the stress-tolerant one multiple times independently (and there is no initial lag). These results confirm the prediction made in Figure S21 that the coexistence of two strategies is promoted by a wider range of conditions than simply those where branching (i.e. divergence in sympatry) occurs.
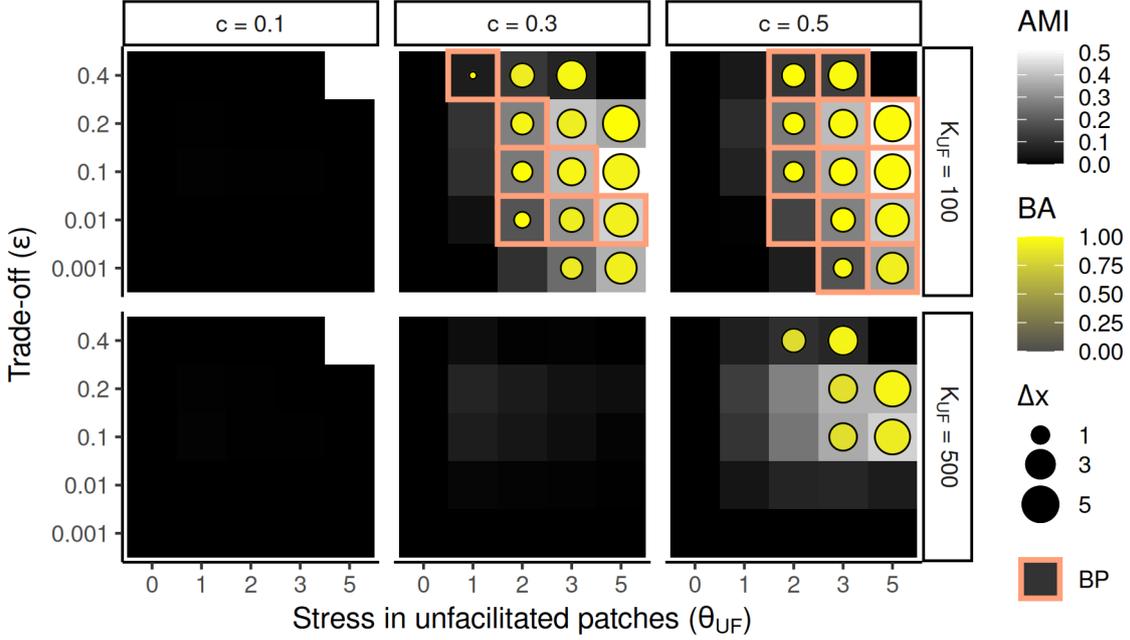
Figure S21: Ability of two morphs to coexist across parameter space. For each combination of parameters, we perform a coexistence analysis as described in Figure S2 (see also Methods). We first determine the *area of mutual invasibility* (AMI), i.e. the proportion of all possible pairs of tolerance strategies, or morphs, that could mutually invade each other in an adaptive dynamics analysis. These are all the pairs of strategies in phenotype space that can in principle coexist, at least on the short term (an AMI of 0 meaning that no coexistence of any two morphs is possible). Following up, we identify stable equilibrium coalitions of morphs, which are pairs of strategies that not only can coexist, but which long-term evolution will also lead to (they are attractors of the dimorphic evolutionary dynamics, see Fig. S2). For each parameter combination where a stable equilibrium coalition is found to exist (circles within tiles), we measure its basin of attraction (BA), the proportion of all pairs of strategies within the AMI that are expected to converge towards that equilibrium coalition during evolution. Tiles where no stable equilibrium coalition is found but still some pairs of strategies are mutually invasible (AMI > 0) are cases where coexistence is in theory possible on the short term, but will be lost if morphs are allowed to evolve (as one will end up outcompeting the other). Hence, while the AMI is a proxy for the propensity of the model to allow the coexistence of two morphs on an ecological time scale, given some parameter values, the BA measures how prone selection is to maintain such coexistence over evolutionary time (see Fig. S2 for details about how these metrics are computed). The size of the circles within the tiles indicates the phenotypic distance between the stress tolerance values of the two morphs at the identified equilibrium coalition ($\Delta x \simeq 5$ being approximately the distance found between the stress-tolerant strategy and the stress-sensitive strategy in Fig. 3A). Finally, orange squares identify parameter combinations where a branching point was found (see Fig. S19), highlighting that branching points are not always needed for transient coexistence (AMI > 0) or its long-term maintenance (BA > 0) in this model (see Fig. S20). Parameters not mentioned in this figure are as per Fig. 3.
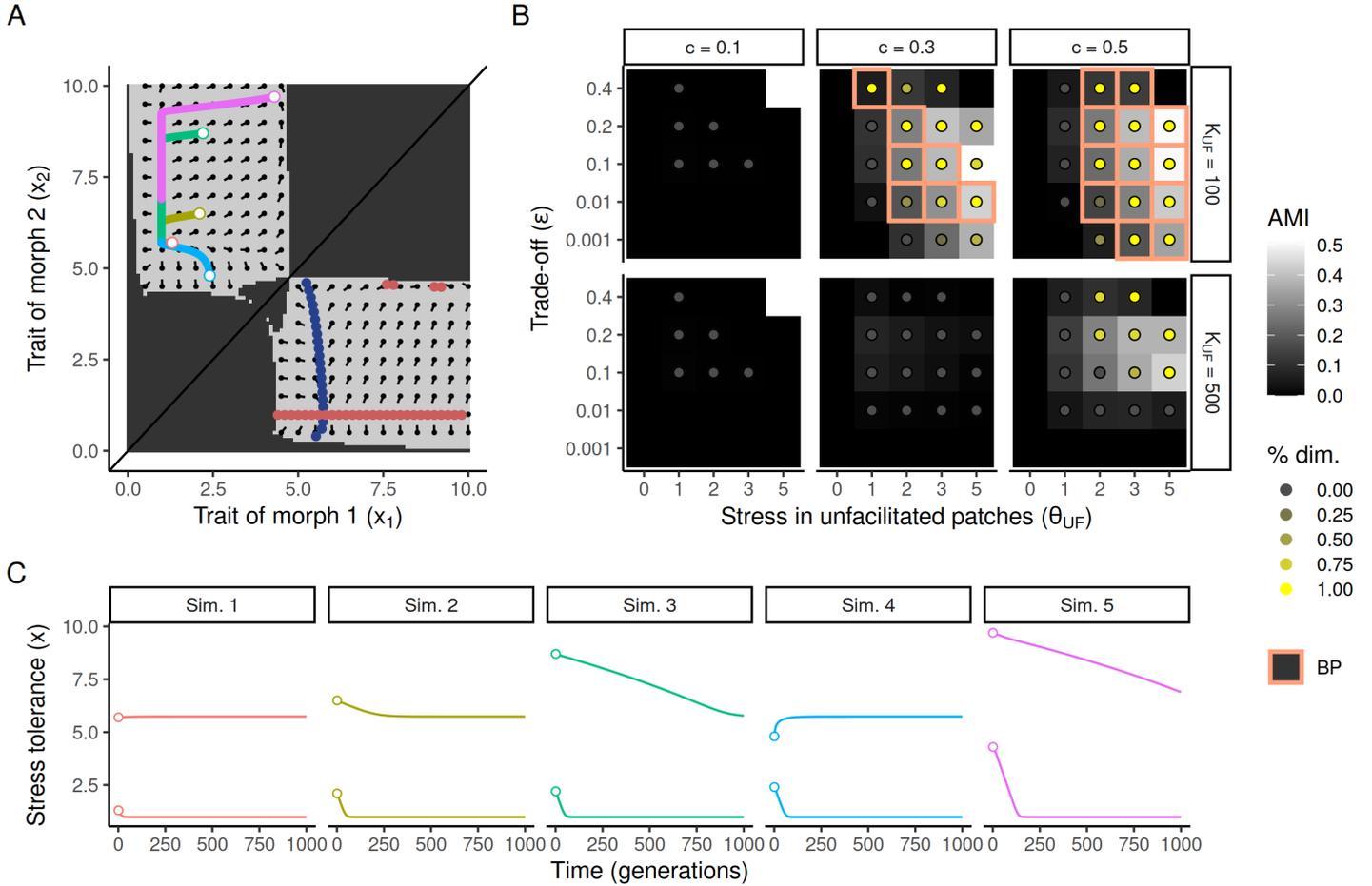
Figure S22: Simulation-based coexistence analysis. In this analysis, we validate the predictions of the adaptive dynamics analysis shown in Fig. S21. (A) For each combination of parameters, we ran five simulations of a deterministic version of our model with two morphs (colored lines above the diagonal, see Appendix for details of the deterministic simulations), starting at randomly sampled points within the area of mutual invasibility (AMI) (white circles within the light gray area, see Fig. S2). The proportion of simulations converging towards a dimorphic, stable equilibrium coalition (such as the crossing between the blue and red isoclines below the diagonal) are shown in B. (B) Results of the analysis, the same as in Fig. S21, but where the potential for coexistence is measured as the proportion of simulations that remained dimorphic rather than using predicted basins of attraction. Simulations that did not remain dimorphic are simulations that went out of the AMI (e.g. into the dark gray zone in A), and one morph outcompeted the other. (C) Trait values of the two morphs in the deterministic simulations shown in A, all converging to the same equilibrium coalition. Parameters specific to the deterministic model: $\mu_x = 0.01$ and $\sigma_x = 0.5$. The mutual invasibility plot (MIP) shown in A is the same as in Fig. S2.
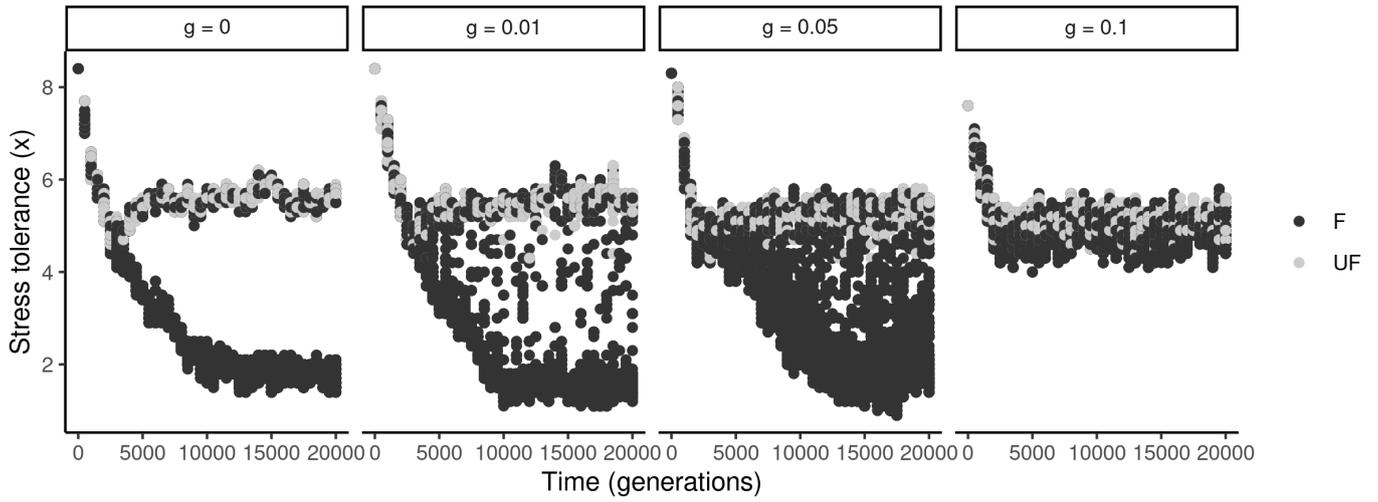
Figure S23: Simulations across levels of outcrossing g. The parameters were chosen to promote branching of an initially highly tolerant population into a stress-sensitive and a stress-tolerant strategy ($K_{UF} = 100$, $p_0 = 0.8$, all other parameters as in Fig. 3). The leftmost panel (pure selfing, $g = 0$) shows that this only holds in the absence of gene flow, as increasing outcrossing even to low levels (g being the proportion of flowers fecundated by a pollen grain, see Methods) already breaks down diversity and homogenizes the population into one, relatively stress-tolerant, morph.
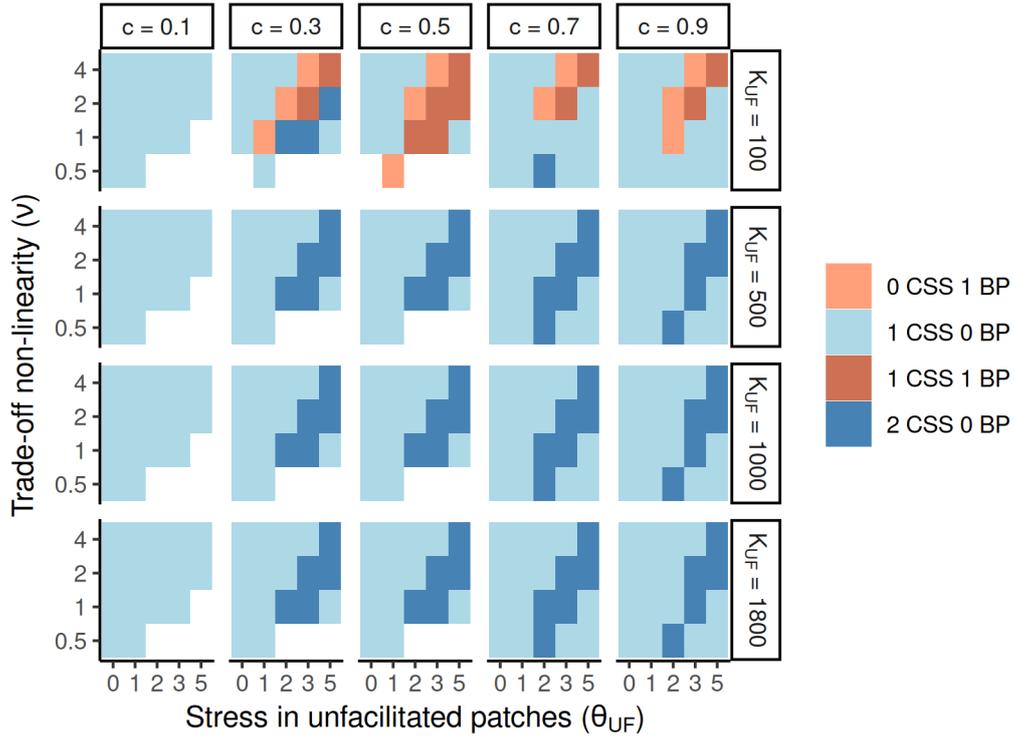
Figure S24: Types of evolutionary equilibria across parameter space when the trade-off between stress tolerance and reproductive output is non-linear. The procedure is the same as in Figure S19, except the trade-off strength parameter is fixed at $\epsilon = 0.4$, and the non-linearity parameter ν is varied instead (all other parameters as per Fig. 3). The results largely overlap with the linear case (Fig. S19), but note that the image must be flipped to see that, as higher ν means a more concave trade-off curve (see Fig. 1C), and so a more shallow decrease in fecundity at low values of stress tolerance (as opposed to higher ϵ, which means a steeper decline), and vice versa for lower ν.
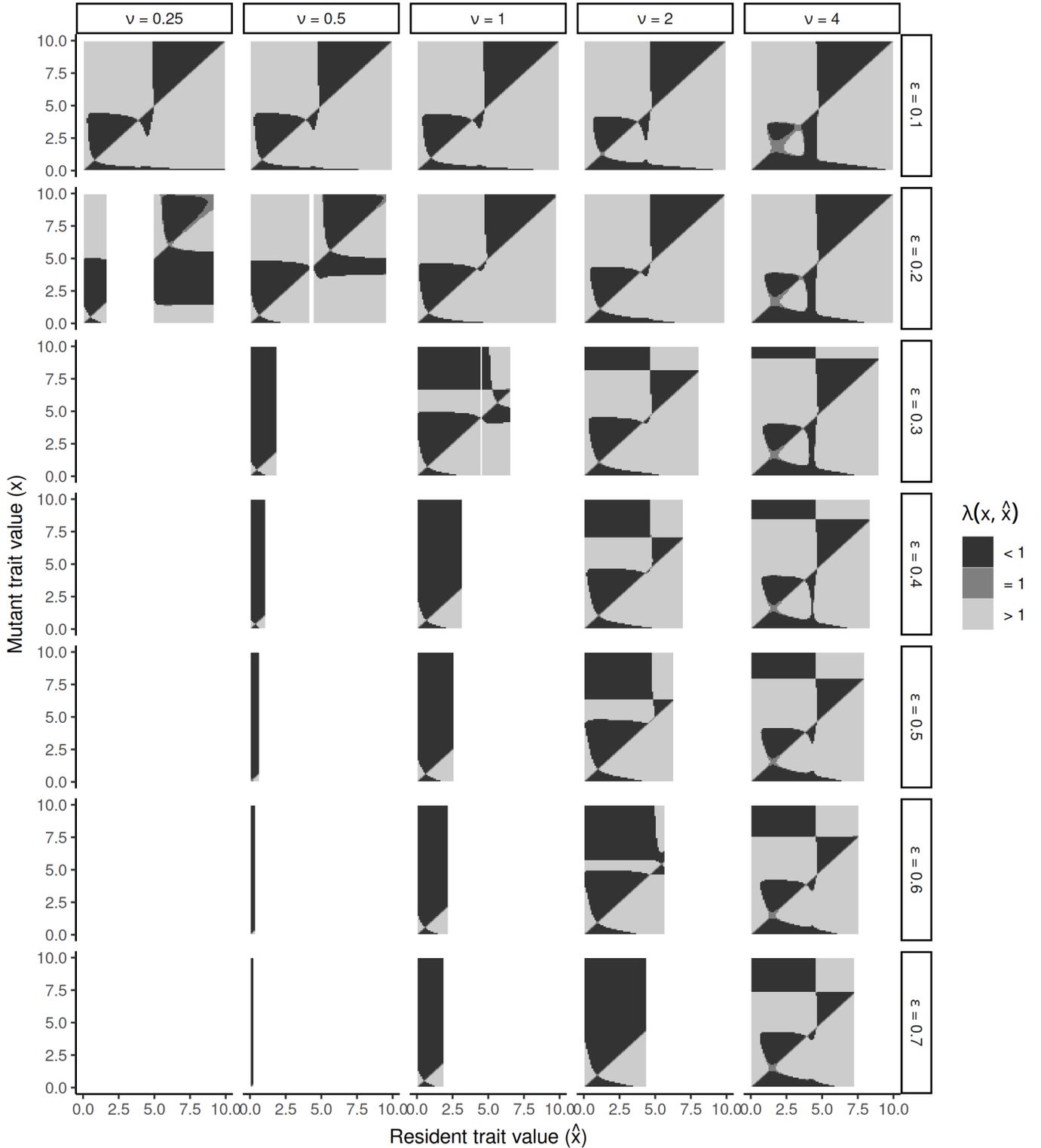
Figure S25: Effects of trade-off non-linearity ν and trade-off strength ϵ on the adaptive dynamics of the model. Other parameters are as per Fig. 3 (except $K_{\mathrm{UF}} = 100$). Note that a higher ν (i.e. more concave trade-off) tends to recover the viable trait space that is otherwise lost when ϵ increases (i.e. the linear component of the trade-off becomes steeper), by making the decrease in reproductive output with stress tolerance relatively shallow, at least as long as stress tolerance is not too close to its maximum x_{max}. In comparison, the effect of ν is negligible when the trade-off is weak (e.g. $\epsilon = 0.1$), as the decrease in reproductive output is shallow enough for its convexity or concavity not to matter too much.

Appendix

In this appendix, we go over the approximation model we designed to accompany our stochastic simulations (see Methods). We study this deterministic version of the model with adaptive dynamics theory, a body of mathematical tools making use of simplifying assumptions (e.g. no genetic drift, separation of time scales and monomorphic populations) to get insights into the role of selection (in contrast with other factors such as stochasticity or genetic architecture) on the evolutionary dynamics of a particular system (Metz et al., 1992, 1996; Geritz et al., 1998). The formulas presented here were independently tested using the mathematical computing software *Mathematica*, version 12.1 (Wolfram Reasearch, Inc.). Numerical evaluations of relevant quantities were performed using R 4.3.3 (R Core Team, 2025), with a C++ backend (integrated into the R environment with Rcpp 1.0.12, Eddelbuettel et al., 2024) for the iterative computation of demographic equilibria (see accompanying code).

Demographic model First, we must determine the demographic dynamics of a rare *mutant* with trait value x (hereafter, the mutant trait value) arising in an otherwise monomorphic population of *resident* individuals with trait value $\hat{x}$ (hereafter, the resident trait value). The demographics of the mutant can be described by the deterministic recursion

$$\overrightarrow{N}_{t+1} = \mathbf{\Lambda}(x, \hat{x}) \, \overrightarrow{N}_t \tag{4}$$

where $\overrightarrow{N}_t$ is a vector containing the numbers of mutant individuals in each patch at time t,

$$\overrightarrow{N}_t = \begin{pmatrix} N_{\mathrm{F}} \\ N_{\mathrm{UF}} \end{pmatrix}_t \tag{5}$$

(in this simplification we assume only one site, $n_{\mathrm{D}} = 1$), and $\mathbf{\Lambda}$ is a transition matrix from t to $t+1$. This transition matrix represents the life cycle of the organism and is given by

$$\mathbf{\Lambda}(x, \hat{x}) = \boldsymbol{S}(x) \, \boldsymbol{M} \, \boldsymbol{R}(x, \hat{x}) \tag{6}$$

where $\boldsymbol{R}$ is the reproduction matrix, $\boldsymbol{M}$ is the (between-patch) migration matrix, and $\boldsymbol{S}$ is the survival matrix. These matrices are the steps of the life cycle and are multiplied with the population vector $\overrightarrow{N}_t$, from right to left. Hence, the life cycle starts with the generation of seeds, determined by the reproduction matrix,

$$\boldsymbol{R}(x, \hat{x}) = \begin{pmatrix} r_{\mathrm{F}}(x, \hat{x}) & 0 \\ 0 & r_{\mathrm{UF}}(x, \hat{x}) \end{pmatrix} \tag{7}$$

where $r_j(x)$ is the reproductive output of an individual from patch j (F or UF) with trait value x, given by

$$r_j(x, \hat{x}) = \exp\left[y(x) \left(1 - \frac{\hat{N}_j^*(\hat{x})}{C_j \, K_j} \right) \right] \tag{8}$$

57

where

$$y(x) = r_{\max} - \epsilon\, x \left(x/x_{\max}\right)^{\nu-1} , \tag{9}$$

just as in Equations 1 and 2 (see Methods), except that here $\hat{N}_j^*$ represents the equilibrium population density of a resident with trait value $\hat{x}$ (we assume that the density of mutants N_j is negligible). Same as in the stochastic version of our model, we have $C_{\mathrm{F}} = c$ and $C_{\mathrm{UF}} = 1 - c$, where c is the shrub cover in the environment. Other parameters and variables are as explained in the Methods.

Reproduction is followed by dispersal between the (F and UF) patches, according to the migration matrix,

$$\boldsymbol{M} = \begin{pmatrix} c & c \\ 1-c & 1-c \end{pmatrix} \tag{10}$$

which corresponds to free dispersal of seeds within the site (the seeds join a common pool and are then distributed into the two patches proportionally to their relative cover, c or $1 - c$, irrespective of patch of origin).

Once landed, successful seed germination is determined by the survival matrix,

$$\boldsymbol{S}(x) = \begin{pmatrix} s_{\mathrm{F}}(x) & 0 \\ 0 & s_{\mathrm{UF}}(x) \end{pmatrix} \tag{11}$$

where $s_j(x)$ is the probability of survival of an individual with trait value x in patch j, given by

$$s_j(x) = \frac{1}{1 + \exp[a\,(\theta_j - x)]} \tag{12}$$

(just like in Eq. 3).

Invasion fitness Next, we conduct an *invasion analysis* to know whether a given mutant x will invade, and replace, its resident competitor $\hat{x}$, or disappear, before the next mutant enters the scene — adaptive dynamics assumes a separation of time scales between ecological and evolutionary processes, such that the demographics reach their equilibrium fast relative to the appearance of new mutations. This is done by calculating the so-called *invasion fitness* λ of the mutant given the resident. Following Otto and Day (2007), the invasion fitness can be derived as the leading eigenvalue of the transition matrix $\boldsymbol{\Lambda}$ of the mutant, which in this case is

$$\lambda(x, \hat{x}) = c\, r_{\mathrm{F}}(x, \hat{x})\, s_{\mathrm{F}}(x) + (1 - c)\, r_{\mathrm{UF}}(x, \hat{x})\, s_{\mathrm{UF}}(x) . \tag{13}$$

The mutant will invade and become the new resident if its invasion fitness is above one ($\lambda > 1$).

Resident equilibrium density The separation of time scales also means that $\hat{N}_j^*(\hat{x})$ is the equilibrium population density reached by the resident population before the introduction of a

new mutant. This equilibrium density must be known in order to compute the invasion fitness. It can be found by solving the system of equations

$$\overrightarrow{N}_t = \mathbf{\Lambda}(\hat{x}, \hat{x}) \, \overrightarrow{N}_t \, , \tag{14}$$

that is, finding the steady state at which the density of the resident no longer changes through ecological time. However, because $\mathbf{\Lambda}(\hat{x}, \hat{x})$ is not independent of $\hat{N}_{\mathrm{F}}$ and $\hat{N}_{\mathrm{UF}}$ (the components of $\overrightarrow{N}$), we did not find this solution analytically. Instead, we computed the equilibrium density vector using long-term iteration of the demographic dynamics, starting with low initial densities (see accompanying code for details).

Once the invasion fitness computed, it can be used to visualize which mutant strategies can invade which resident ones. Such graphical representations, called *pairwise invasibility plots*, can help identify evolutionary steady states, or *singularities*, which in some cases are the predicted endpoints of evolution through successive invasions (see Fig. S1).

Selection gradient   It is also possible to derive a *selection gradient* from the invasion fitness function. The selection gradient represents the direction and magnitude of selection operating on the evolving trait during evolution through successive invasions. This means that evolutionary singularities are resident strategies where the selection gradient is zero — solving this equation can therefore help find singularities without having to calculate invasion fitness for thousands of mutant-resident pairs. The selection gradient can also be used to run evolutionary simulations according to the deterministic version of the model, and compare them to stochastic individual-based simulations.

Mathematically, the selection gradient $G(\hat{x})$ is the derivative of the invasion fitness λ with respect to the mutant trait value x, evaluated at the resident strategy $\hat{x}$ (i.e. when the mutant has the same trait value as the resident, $x = \hat{x}$). For our model, this corresponds to

$$
\begin{aligned}
G(\hat{x}) = \left. \frac{\partial \lambda}{\partial x} \right|_{x=\hat{x}} = {} & c \left(\hat{r}'_{\mathrm{F}}(\hat{x}) \, s_{\mathrm{F}}(\hat{x}) + \hat{r}_{\mathrm{F}}(\hat{x}) \, \hat{s}'_{\mathrm{F}}(\hat{x}) \right) \\
& + (1 - c) \left(\hat{r}'_{\mathrm{UF}}(\hat{x}) \, s_{\mathrm{UF}}(\hat{x}) + \hat{r}_{\mathrm{UF}}(\hat{x}) \, \hat{s}'_{\mathrm{UF}}(\hat{x}) \right)
\end{aligned}
\tag{15}
$$

where $\hat{r}_j(\hat{x}) = r_j(\hat{x}, \hat{x})$, $\hat{r}'_j(\hat{x}) = \partial r_j / \partial x|_{x=\hat{x}}$ and $\hat{s}'_j(\hat{x}) = \partial s_j / \partial x|_{x=\hat{x}}$, with

$$\frac{\partial s_j}{\partial x} = a \, s_j(x) \left(1 - s_j(x) \right) \tag{16}$$

and

$$\frac{\partial r_j}{\partial x} = \left(1 - \frac{N_j^*(\hat{x})}{C_j \, K_j} \right) \frac{\partial y}{\partial x} \, r_j(x, \hat{x}) \tag{17}$$

where

$$\frac{\partial y}{\partial x} = -\epsilon \, \nu \, x_{\max}^{1-\nu} \, x^{\nu-1} \, . \tag{18}$$

Numerical simulations Because the selection gradient $G(\hat{x})$ is a function of the resident trait $\hat{x}$ and not of the mutant trait x anymore, we can use it to simulate the expected change in resident trait value through evolutionary time given some parameter values, without explicitly modeling the mutants. In our deterministic evolutionary simulations, the change in trait from one (evolutionary) time point to the next is given by

$$\hat{x}_{t+1} = \hat{x}_t + \text{1/2} \, N_t \, \mu_x \, \sigma_x^2 \, G(\hat{x}_t) \tag{19}$$

where N_t is the total population size at time t, μ_x is the trait-wide mutation rate of trait x (as opposed to a locus-specific mutation rate μ used in the individual-based model, see Methods) and σ_x is the mutational standard deviation, which controls the magnitude of phenotypic change brought about by mutations (see Table **??** for the default values of these parameters). Note that models studied with adaptive dynamics are phenotypic models, which must assume a simple genetic basis of traits in order to be mathematically tractable (Metz et al., 1996; Geritz et al., 1998). Here, the phenotype is assumed to be encoded by a single haploid locus with an infinite continuum of quantitative alleles, where the phenotypic effects of mutations occurring at rate μ_x are normally distributed with standard deviation σ_x.

Evolutionary stability It is possible to determine the evolutionary stability of a singular strategy (i.e. whether once reached, no mutants can invade) by studying the sign of the curvature of the invasion fitness function, evaluated at that singular strategy. If the curvature is negative, the singularity is a fitness 'peak' — no mutant in close phenotypic proximity can invade, and the strategy is evolutionarily stable. If the curvature is positive, the singular strategy is an unstable evolutionary equilibrium.

The fitness curvature F at a singularity x^* is the second derivative of the fitness function evaluated at that resident strategy, i.e.,

$$\begin{aligned} F(x^*) = \left.\frac{\partial^2 \lambda}{\partial x^2}\right|_{x=\hat{x}=x^*} &= c \left(\hat{r}_{\mathrm{F}}''(x^*) \, s_{\mathrm{F}}(x^*) + 2 \, \hat{r}_{\mathrm{F}}'(x^*) \, \hat{s}_{\mathrm{F}}'(x^*) + \hat{r}_{\mathrm{F}}(x^*) \, \hat{s}_{\mathrm{F}}''(x^*) \right) \\ &+ (1-c) \left(\hat{r}_{\mathrm{UF}}''(x^*) \, s_{\mathrm{UF}}(x^*) + 2 \, \hat{r}_{\mathrm{UF}}'(x^*) \, \hat{s}_{\mathrm{UF}}'(x^*) + r_{\mathrm{UF}}(x^*) \, \hat{s}_{\mathrm{UF}}''(x^*) \right) \end{aligned} \tag{20}$$

where $\hat{r}_j''(x^*) = \partial^2 r_j / \partial x^2|_{x=x^*}$ and $\hat{s}_j''(x^*) = \partial^2 s_j / \partial x^2|_{x=x^*}$, with

$$\frac{\partial^2 s_j}{\partial x^2} = a \left(1 - 2 \, s_j(x) \right) \frac{\partial s_j}{\partial x} \tag{21}$$

and

$$\frac{\partial^2 r_j}{\partial x^2} = \epsilon \left(1 - \frac{\hat{N}_j^*(\hat{x})}{C_j \, K_j} \right) \left(\frac{\partial y}{\partial x} \frac{\partial r_j}{\partial x} + r_j(x, \hat{x}) \frac{\partial^2 y}{\partial x^2} \right) \tag{22}$$

60

where

$$\frac{\partial y}{\partial x} = -\epsilon \, \nu \, x_{\max}^{1-\nu} \, x^{\nu-1} \tag{23}$$

and

$$\frac{\partial^2 y}{\partial x^2} = -\epsilon \, \nu \, (\nu - 1) \, x_{\max}^{1-\nu} \, x^{\nu-2} \; . \tag{24}$$

Convergence stability The convergence stability of a singular strategy, i.e. whether evolution leads towards it (independently of whether it is evolutionarily stable once reached, see above), can be determined by looking at whether the selection gradient points towards that singularity from nearby resident strategies. This is equivalent to studying how the sign of the selection gradient $G(\hat{x})$ changes as the resident strategy $\hat{x}$ varies and goes through the putative equilibrium strategy that the singularity x^* represents, which is given by the sign of

$$H(x^*) = \left. \frac{\partial G}{\partial \hat{x}} \right|_{\hat{x}=x^*} \; . \tag{25}$$

If H is negative, the selection gradient is positive for $\hat{x} < x^*$ and negative for $\hat{x} > x^*$, meaning that the singular strategy x^* is a local attractor of the adaptive dynamics — it is convergence stable. If H is positive, selection leads away from x^*, and x^* is convergence unstable.

Because calculating H involves differentiating $\hat{N}_j$ with respect to $\hat{x}$, we could not find it analytically, for the same reason that we had to compute $\hat{N}_j$ numerically (see section on equilibrium resident density above). Instead, we measured H numerically, by computing the selection gradient G on each side of the equilibrium and looking at the sign of the difference (details available in the accompanying code).

Dimorphic evolution Some types of evolutionary singularities are convergence stable but evolutionarily unstable. These are called *branching points* (see Fig. S1), and can cause a monomorphic population to split into two coevolving morphs, each with their own adaptive dynamics. Once such branching happens, the monomorphic model no longer describes the dynamics of the system, and must be updated to keep track of the adaptive dynamics of the two morphs. In the updated model, each morph k with mutant trait value x_k and resident trait values $\hat{x}_k$ and $\hat{x}_l$ (l referring to the other morph) has its own transition matrix $\boldsymbol{\Lambda}_{\dim}(x_k, \hat{x}_k, \hat{x}_l) = \boldsymbol{S}(x_k) \, \boldsymbol{M} \, \boldsymbol{R}_{\dim}(x_k, \hat{x}_k, \hat{x}_l)$, where the migration matrix $\boldsymbol{M}$ and the survival matrix $\boldsymbol{S}$ have not changed, but where the (dimorphic) reproduction matrix is now

$$\boldsymbol{R}_{\dim}(x_k, \hat{x}_k, \hat{x}_l) = \begin{pmatrix} r_{\mathrm{F}}^{\dim}(x_k, \hat{x}_k, \hat{x}_l) & 0 \\ 0 & r_{\mathrm{F}}^{\dim}(x_k, \hat{x}_k, \hat{x}_l) \end{pmatrix} \tag{26}$$

where

$$r_j^{\dim}(x_k, \hat{x}_k, \hat{x}_l) = \exp\left[y(x_k)\left(1 - \frac{\hat{N}_{jk}^*(\hat{x}_k, \hat{x}_l) + \hat{N}_{jl}^*(\hat{x}_k, \hat{x}_l)}{C_j\,K_j}\right)\right] \tag{27}$$

where

$$y = r_{\max} - \epsilon\,x\,(x/x_{\max})^{\nu-1} \tag{28}$$

where $\hat{N}_{jk}^*(\hat{x}_k, \hat{x}_l) + \hat{N}_{jl}^*(\hat{x}_k, \hat{x}_l)$ symbolizes the fact that any individual experiences density dependence from both morphs in its local patch j.

The invasion fitness of a mutant is now given by

$$\lambda_{\dim}(x_k, \hat{x}_k, \hat{x}_l) = c\,r_{\mathrm{F}}^{\dim}(x_k, \hat{x}_k, \hat{x}_l)\,s_{\mathrm{F}}(x_k) + (1-c)\,r_{\mathrm{UF}}^{\dim}(x_k, \hat{x}_k, \hat{x}_l)\,s_{\mathrm{UF}}(x_k) \tag{29}$$

and the morph-specific selection gradient (obtained, for each morph k, by differentiating the invasion fitness while keeping the other morph constant) becomes

$$\begin{aligned}
G_k(\hat{x}_k, \hat{x}_l) = \left.\frac{\partial\lambda_k}{\partial x_k}\right|_{x_k=\hat{x}_k} &= c\left(\hat{r}_{\mathrm{F}}'^{\dim}(\hat{x}_k, \hat{x}_l)\,s_{\mathrm{F}}(\hat{x}_k) + \hat{r}_{\mathrm{F}}^{\dim}(\hat{x}_k, \hat{x}_l)\,\hat{s}_{\mathrm{F}}'(\hat{x}_k)\right)\\
&+ (1-c)\left(\hat{r}_{\mathrm{UF}}'^{\dim}(\hat{x}_k, \hat{x}_l)\,s_{\mathrm{UF}}(\hat{x}_k) + \hat{r}_{\mathrm{UF}}^{\dim}(\hat{x}_k, \hat{x}_l)\,\hat{s}_{\mathrm{UF}}'(\hat{x}_k)\right)
\end{aligned} \tag{30}$$

where $\hat{r}_j'^{\dim}(\hat{x}_k, \hat{x}_l) = \partial r_j^{\dim}/\partial x_k|_{x_k=\hat{x}_k}$. The two-dimensional dimorphic selection gradient vector is then given by

$$\overrightarrow{G}_{\dim}(\hat{x}_k, \hat{x}_l) = \begin{pmatrix} G_k(\hat{x}_k, \hat{x}_l) \\ G_l(\hat{x}_l, \hat{x}_k) \end{pmatrix}. \tag{31}$$

References

Adler, P. B., Smull, D., Beard, K. H., Choi, R. T., Furniss, T., Kulmatiski, A., Meiners, J. M., Tredennick, A. T., & Veblen, K. E. (2018). Competition and coexistence in plant communities: Intraspecific competition is stronger than interspecific competition. *Ecology Letters*, *21*(9), 1319–1329. https://doi.org/10.1111/ele.13098

Aguilée, R., Raoul, G., Rousset, F., & Ronce, O. (2016). Pollen dispersal slows geographical range shift and accelerates ecological niche shift under climate change. *Proceedings of the National Academy of Sciences*, *113*(39), E5741–E5748. https://doi.org/10.1073/pnas.1607612113

Aguilera, M. A., Valdivia, N., & Broitman, B. R. (2015). Facilitative effect of a generalist herbivore on the recovery of a perennial alga: Consequences for persistence at the edge of their geographic range. *PLOS ONE*, *10*(12), e0146069. https://doi.org/10.1371/journal.pone.0146069

Alfaro, M., Berestycki, H., & Raoul, G. (2017). The effect of climate shift on a species submitted to dispersion, evolution, growth, and nonlocal competition. *SIAM Journal on Mathematical Analysis*, *49*(1), 562–596. https://doi.org/10.1137/16M1075934

Alleaume-Benharira, M., Pen, I. R., & Ronce, O. (2006). Geographical patterns of adaptation within a species' range: Interactions between drift and gene flow. *Journal of Evolutionary Biology*, *19*(1), 203–215. https://doi.org/10.1111/j.1420-9101.2005.00976.x

Angert, A. L., Bontrager, M. G., & Ågren, J. (2020). What do we really know about adaptation at range edges? *Annual Review of Ecology, Evolution, and Systematics*, *51*(Volume 51, 2020), 341–361. https://doi.org/10.1146/annurev-ecolsys-012120-091002

Arenas, M., Ray, N., Currat, M., & Excoffier, L. (2012). Consequences of range contractions and range shifts on molecular diversity. *Molecular Biology and Evolution*, *29*(1), 207–218. https://doi.org/10.1093/molbev/msr187

Armas, C., Pugnaire, F. I., & Sala, O. E. (2008). Patch structure dynamics and mechanisms of cyclical succession in a Patagonian steppe (Argentina). *Journal of Arid Environments*, *72*(9), 1552–1561. https://doi.org/10.1016/j.jaridenv.2008.03.002

Armas, C., & Pugnaire, F. I. (2005). Plant interactions govern population dynamics in a semi-arid plant community. *Journal of Ecology*, *93*(5), 978–989. https://doi.org/10.1111/j.1365-2745.2005.01033.x

Armas, C., Rodríguez-Echeverría, S., & Pugnaire, F. I. (2011). A field test of the stress-gradient hypothesis along an aridity gradient. *Journal of Vegetation Science*, *22*(5), 818–827. https://doi.org/10.1111/j.1654-1103.2011.01301.x

Badyaev, A. V. (2005). Stress-induced variation in evolution: From behavioural plasticity to genetic assimilation. *Proceedings of the Royal Society B: Biological Sciences*, *272*(1566), 877–886. https://doi.org/10.1098/rspb.2004.3045

Barton, N. H. (2001). Adaptation at the edge of a species' range. In *Integrating ecology and evolution in a spatial context* (pp. 365–392). Blackwell.

Bell, G. (2017). Evolutionary rescue. *Annual Review of Ecology, Evolution, and Systematics*, *48*(Volume 48, 2017), 605–627. https://doi.org/10.1146/annurev-ecolsys-110316-023011

Bell, G., & Collins, S. (2008). Adaptation, extinction and global change. *Evolutionary Applications*, *1*(1), 3–16. https://doi.org/10.1111/j.1752-4571.2007.00011.x

Bertness, M. D., & Callaway, R. (1994). Positive interactions in communities. *Trends in Ecology & Evolution*, *9*(5), 191–193.

Boulding, E. G., & Hay, T. (2001). Genetic and demographic parameters determining population persistence after a discrete change in the environment. *Heredity*, *86*(3), 313–324. https://doi.org/10.1046/j.1365-2540.2001.00829.x

Bridle, J. R., Polechová, J., Kawata, M., & Butlin, R. K. (2010). Why is adaptation prevented at ecological margins? New insights from individual-based simulations. *Ecology Letters*, *13*(4), 485–494. https://doi.org/10.1111/j.1461-0248.2010.01442.x

Bridle, J. R., & Vines, T. H. (2007). Limits to evolution at range margins: When and why does adaptation fail? *Trends in Ecology & Evolution*, *22*(3), 140–147. https://doi.org/10.1016/j.tree.2006.11.002

Brooker, R. W. (2006). Plant–plant interactions and environmental change. *New Phytologist*, *171*(2), 271–284. https://doi.org/10.1111/j.1469-8137.2006.01752.x

Brown, J. S., & Pavlovic, N. B. (1992). Evolution in heterogeneous environments: Effects of migration on habitat specialization. *Evolutionary Ecology*, *6*(5), 360–382. https://doi.org/10.1007/BF02270698

Bruno, J. F., Stachowicz, J. J., & Bertness, M. D. (2003). Inclusion of facilitation into ecological theory. *Trends in Ecology & Evolution*, *18*(3), 119–125. https://doi.org/10.1016/S0169-5347(02)00045-9

Bulleri, F. (2009). Facilitation research in marine systems: State of the art, emerging patterns and insights for future developments. *Journal of Ecology*, *97*(6), 1121–1130. https://doi.org/10.1111/j.1365-2745.2009.01567.x

Bürger, R., & Lynch, M. (1995). Evolution and extinction in a changing environment: A quantitative-genetic analysis. *Evolution*, *49*(1), 151–163. https://doi.org/10.1111/j.1558-5646.1995.tb05967.x

Callaway, R. M. (2007a). Interaction between competition and facilitation. In *Positive interactions and interdependence in plant communities* (pp. 179–254). Springer.

Callaway, R. M. (2007b). *Positive interactions and interdependence in plant communities*. Springer.

Case, T. J., Holt, R. D., McPeek, M. A., & Keitt, T. H. (2005). The community context of species' borders: Ecological and evolutionary perspectives. *Oikos*, *108*(1), 28–46. https://doi.org/10.1111/j.0030-1299.2005.13148.x

Case, T. J., & Taper, M. L. (2000). Interspecific competition, environmental gradients, gene flow, and the coevolution of species' borders. *The American Naturalist*, *155*(5), 583–605. https://doi.org/10.1086/303351

Chevin, L.-M., & Lande, R. (2011). Adaptation to marginal habitats by evolution of increased phenotypic plasticity. *Journal of Evolutionary Biology*, *24*(7), 1462–1476. https://doi.org/10.1111/j.1420-9101.2011.02279.x

Chevin, L.-M., & Hoffmann, A. A. (2017). Evolution of phenotypic plasticity in extreme environments. *Philosophical Transactions of the Royal Society B: Biological Sciences*, *372*(1723), 20160138. https://doi.org/10.1098/rstb.2016.0138

Chevin, L.-M., Lande, R., & Mace, G. M. (2010). Adaptation, plasticity, and extinction in a changing environment: Towards a predictive theory. *PLOS Biology*, *8*(4), e1000357. https://doi.org/10.1371/journal.pbio.1000357

Crombach, A., & Hogeweg, P. (2008). Evolution of evolvability in gene regulatory networks (H. M. Sauro, Ed.). *PLOS Computational Biology*, *4*(7), e1000112. https://doi.org/10.1371/journal.pcbi.1000112

Day, R. L., Laland, K. N., & Odling-Smee, F. J. (2003). Rethinking adaptation: The niche-construction perspective. *Perspectives in Biology and Medicine*, *46*(1), 80–95.

de Mazancourt, C., & Dieckmann, U. (2004). Trade-off geometries and frequency-dependent selection. *The American Naturalist*, *164*(6), 765–778. https://doi.org/10.1086/424762

D'Odorico, P., Bhattachan, A., Davis, K. F., Ravi, S., & Runyan, C. W. (2013). Global desertification: Drivers and feedbacks. *Advances in Water Resources*, *51*, 326–344. https://doi.org/10.1016/j.advwatres.2012.01.013

Duputié, A., Massol, F., Chuine, I., Kirkpatrick, M., & Ronce, O. (2012). How do genetic correlations affect species range shifts in a changing environment? *Ecology Letters*, *15*(3), 251–259. https://doi.org/10.1111/j.1461-0248.2011.01734.x

Eddelbuettel, D., François, R., Allaire, J., Ushey, K., Kou, Q., Russel, N., Ucar, I., Bates, D., & Chambers, J. (2024). Rcpp: Seamless R and C++ integration.

Filin, I., Holt, R. D., & Barfield, M. (2008). The relation of density regulation to habitat specialization, evolution of a species' range, and the dynamics of biological invasions. *The American Naturalist*, *172*(2), 233–247. https://doi.org/10.1086/589459

Flatt, T. (2005). The evolutionary genetics of canalization. *The Quarterly Review of Biology*, *80*(3), 287–316. https://doi.org/10.1086/432265

Franklin, J., Serra-Diaz, J. M., Syphard, A. D., & Regan, H. M. (2016). Global change and terrestrial plant community dynamics. *Proceedings of the National Academy of Sciences*, *113*(14), 3725–3734. https://doi.org/10.1073/pnas.1519911113

Gandon, S., & Michalakis, Y. (2002). Local adaptation, evolutionary potential and host–parasite coevolution: Interactions between migration, mutation, population size and generation time. *Journal of Evolutionary Biology*, *15*(3), 451–462. https://doi.org/10.1046/j.1420-9101.2002.00402.x

García-Ramos, G., & Huang, Y. (2013). Competition and evolution along environmental gradients: Patterns, boundaries and sympatric divergence. *Evolutionary Ecology*, *27*(3), 489–504. https://doi.org/10.1007/s10682-012-9614-y

García-Ramos, G., & Kirkpatrick, M. (1997). Genetic models of adaptation and gene flow in peripheral populations. *Evolution*, *51*(1), 21–28. https://doi.org/10.1111/j.1558-5646.1997.tb02384.x

Geritz, S. A. H., Kisdi, É., Meszéna, G., & Metz, J. A. J. (1998). Evolutionarily singular strategies and the adaptive growth and branching of the evolutionary tree. *Evolutionary Ecology*, *12*(1), 35–57. https://doi.org/10.1023/A:1006554906681

Gibson, G., & Dworkin, I. (2004). Uncovering cryptic genetic variation. *Nature Reviews Genetics*, *5*(9), 681–690. https://doi.org/10.1038/nrg1426

Gilbert, K. J., & Whitlock, M. C. (2017). The genetics of adaptation to discrete heterogeneous environments: Frequent mutation or large-effect alleles can allow range expansion. *Journal of Evolutionary Biology*, *30*(3), 591–602. https://doi.org/10.1111/jeb.13029

Glémin, S., Ronfort, J., & Bataillon, T. (2003). Patterns of inbreeding depression and architecture of the load in subdivided populations. *Genetics*, *165*(4), 2193–2212. https://doi.org/10.1093/genetics/165.4.2193

Gomulkiewicz, R., & Holt, R. D. (1995). When does evolution by natural selection prevent extinction? *Evolution*, *49*(1), 201–207. https://doi.org/10.1111/j.1558-5646.1995.tb05971.x

Gomulkiewicz, R., Holt, R. D., & Barfield, M. (1999). The effects of density dependence and immigration on local adaptation and niche evolution in a black-hole sink environment. *Theoretical Population Biology*, *55*(3), 283–296. https://doi.org/10.1006/tpbi.1998.1405

Gomulkiewicz, R., Holt, R. D., Barfield, M., & Nuismer, S. L. (2010). Genetics, adaptation, and invasion in harsh environments. *Evolutionary Applications*, *3*(2), 97–108. https://doi.org/10.1111/j.1752-4571.2009.00117.x

Gomulkiewicz, R., & Houle, D. (2009). Demographic and genetic constraints on evolution. *The American Naturalist*, *174*(6), E218–E229. https://doi.org/10.1086/645086

Gonzalez, A., Ronce, O., Ferriere, R., & Hochberg, M. E. (2013). Evolutionary rescue: An emerging focus at the intersection between ecology and evolution. *Philosophical Transactions of the Royal Society B: Biological Sciences*, *368*(1610), 20120404. https://doi.org/10.1098/rstb.2012.0404

Hampe, A., & Jump, A. S. (2011). Climate relicts: Past, present, future. *Annual Review of Ecology, Evolution, and Systematics*, *42*(Volume 42, 2011), 313–333. https://doi.org/10.1146/annurev-ecolsys-102710-145015

Hannah, L., Flint, L., Syphard, A. D., Moritz, M. A., Buckley, L. B., & McCullough, I. M. (2014). Fine-grain modeling of species' response to climate change: Holdouts, stepping-stones, and microrefugia. *Trends in Ecology & Evolution*, *29*(7), 390–397. https://doi.org/10.1016/j.tree.2014.04.006

Hendry, A. P. (2017). *Eco-evolutionary dynamics*. Princeton University Press.

Holt, R. D., Gomulkiewicz, R., & Barfield, M. (2003). The phenomenology of niche evolution via quantitative traits in a 'black-hole' sink. *Proceedings of the Royal Society B: Biological Sciences*, *270*(1511), 215–224. https://doi.org/10.1098/rspb.2002.2219

Holt, R. D. (1985). Population dynamics in two-patch environments: Some anomalous consequences of an optimal habitat distribution. *Theoretical Population Biology*, *28*(2), 181–208. https://doi.org/10.1016/0040-5809(85)90027-9

Holt, R. D. (1990). The microevolutionary consequences of climate change. *Trends in Ecology & Evolution*, *5*(9), 311–315. https://doi.org/10.1016/0169-5347(90)90088-U

Holt, R. D. (1996). Demographic constraints in evolution: Towards unifying the evolutionary theories of senescence and niche conservatism. *Evolutionary Ecology*, *10*(1), 1–11. https://doi.org/10.1007/BF01239342

Holt, R. D. (1997). On the evolutionary stability of sink populations. *Evolutionary Ecology*, *11*(6), 723–731. https://doi.org/10.1023/A:1018438403047

Holt, R. D. (2003). On the evolutionary ecology of species' ranges. *Evolutionary Ecology Research*, *5*(2), 159–178.

Holt, R. D., & Barfield, M. (2011). Theoretical perspectives on the statics and dynamics of species' borders in patchy environments. *The American Naturalist*, *178*(S1), S6–S25. https://doi.org/10.1086/661784

Holt, R. D., & Gaines, M. S. (1992). Analysis of adaptation in heterogeneous landscapes: Implications for the evolution of fundamental niches. *Evolutionary Ecology*, *6*(5), 433–447. https://doi.org/10.1007/BF02270702

Holt, R. D., Keitt, T. H., Lewis, M. A., Maurer, B. A., & Taper, M. L. (2005). Theoretical models of species' borders: Single species approaches. *Oikos*, *108*(1), 18–27. https://doi.org/10.1111/j.0030-1299.2005.13147.x

IPCC. (2014). *Climate change 2014 : Mitigation of climate change. Working group III: Contribution to the fifth assessment report of the intergovernmental panel on climate change* (tech. rep.). New York, NY.
Cambridge University Press.

Kawecki, T. J. (1995). Demography of source—sink populations and the evolution of ecological niches. *Evolutionary Ecology*, *9*(1), 38–44. https://doi.org/10.1007/BF01237695

Kawecki, T. J. (2000). Adaptation to marginal habitats: Contrasting influence of the dispersal rate on the fate of alleles with small and large effects. *Proceedings of the Royal Society B: Biological Sciences*, *267*(1450), 1315–1320. https://doi.org/10.1098/rspb.2000.1144

Kawecki, T. J. (2003). Sex-biased dispersal and adaptation to marginal habitats. *The American Naturalist*, *162*(4), 415–426. https://doi.org/10.1086/378048

Kawecki, T. J. (2004, January). Ecological and evolutionary consequences of source-sink population dynamics. In I. Hanski & O. E. Gaggiotti (Eds.), *Ecology, genetics, and evolution of metapopulations* (pp. 387–414). Academic Press. https://doi.org/10.1016/B978-012323448-3/50018-0

Kawecki, T. J. (2008). Adaptation to marginal habitats. *Annual Review of Ecology, Evolution, and Systematics*, *39*, 321–342. https://doi.org/10.1146/annurev.ecolsys.38.091206.095622

Kawecki, T. J., & Holt, R. D. (2002). Evolutionary consequences of asymmetric dispersal rates. *The American Naturalist*, *160*(3), 333–347. https://doi.org/10.1086/341519

Kéfi, S., Baalen, M. v., Rietkerk, M., & Loreau, M. (2008). Evolution of local facilitation in arid ecosystems. *The American Naturalist*, *172*(1), E1–E17. https://doi.org/10.1086/588066

Kimbrell, T., & Holt, R. D. (2007). Canalization breakdown and evolution in a source-sink system. *The American Naturalist*, *169*(3), 370–382. https://doi.org/10.1086/511314

Kinnison, M. T., & Hairston, N. G. (2007). Eco-evolutionary conservation biology: Contemporary evolution and the dynamics of persistence. *Functional Ecology*, *21*(3), 444–454.

Kirkpatrick, M., & Barton, N. H. (1997). Evolution of a species' range. *The American Naturalist*, *150*(1), 1–23. https://doi.org/10.1086/286054

Korte, M. K. (2024). *The angle of response: Facilitation and its effect on the* Brachypodium distachyon *grass complex* [Doctoral dissertation, University of Groningen].

Korte, M. K., Manzaneda, A. J., Martinez, L. M., Patterson, T. A., Etienne, R. S., van de Zande, L., & Smit, C. (2025). The effect of local perennial plants on the occurrence and traits of the *Brachypodium distachyon* complex along an aridity gradient. *Plant Ecology*, *226*(5), 485–495. https://doi.org/10.1007/s11258-025-01508-y

Laland, K., Matthews, B., & Feldman, M. W. (2016). An introduction to niche construction theory. *Evolutionary Ecology*, *30*(2), 191–202. https://doi.org/10.1007/s10682-016-9821-z

Lande, R., & Shannon, S. (1996). The role of genetic variation in adaptation and population persistence in a changing environment. *Evolution*, *50*(1), 434–437. https://doi.org/10.1111/j.1558-5646.1996.tb04504.x

Ledón-Rettig, C. C., Pfennig, D. W., Chunco, A. J., & Dworkin, I. (2014). Cryptic genetic variation in natural populations: A predictive framework. *Integrative and Comparative Biology*, *54*(5), 783–793. https://doi.org/10.1093/icb/icu077

Lenormand, T. (2002). Gene flow and the limits to natural selection. *Trends in Ecology & Evolution*, *17*(4), 183–189. https://doi.org/10.1016/S0169-5347(02)02497-7

Levins, R. A. (1974). *Evolution in changing environments: Some theoretical explorations* (3. printing). Princeton University Press.

Liancourt, P., Choler, P., Gross, N., Thibert-Plante, X., & Tielbörger, K. (2012). How facilitation may interfere with ecological speciation. *International Journal of Ecology*, *2012*(1), 725487. https://doi.org/10.1155/2012/725487

Lopez, S., Rousset, F., Shaw, F. H., Shaw, R. G., & Ronce, O. (2009). Joint effects of inbreeding and local adaptation on the evolution of genetic load after fragmentation. *Conservation Biology*, *23*(6), 1618–1627. https://doi.org/10.1111/j.1523-1739.2009.01326.x

Lortie, C. J., Filazzola, A., Westphal, M., & Butterfield, H. S. (2022). Foundation plant species provide resilience and microclimatic heterogeneity in drylands. *Scientific Reports*, *12*(1), 18005. https://doi.org/10.1038/s41598-022-22579-1

Mellard, J. P., de Mazancourt, C., & Loreau, M. (2015). Evolutionary responses to environmental change: Trophic interactions affect adaptation and persistence. *Proceedings of the Royal Society B: Biological Sciences*, *282*(1805), 20141351. https://doi.org/10.1098/rspb.2014.1351

Metz, J. A. J., Geritz, S. A. H., Meszena, G., Jacobs, F. J. A., & van Heerwaarden, J. S. (1996). Adaptive dynamics: A geometrical study of the consequences of nearly faithful reproduction. In S. J. van Strien & S. M. Verduyn Lunel (Eds.), *Stochastic and spatial structures of dynamical systems* (pp. 183–231).

Metz, J. A. J., Nisbet, R. M., & Geritz, S. A. H. (1992). How should we define 'fitness' for general ecological scenarios? *Trends in Ecology & Evolution*, *7*(6), 198–202. https://doi.org/10.1016/0169-5347(92)90073-K

Michalet, R., Xiao, S., Touzard, B., Smith, D. S., Cavieres, L. A., Callaway, R. M., & Whitham, T. G. (2011). Phenotypic variation in nurse traits and community feedbacks define an

alpine community. *Ecology Letters*, *14*(5), 433–443. https://doi.org/10.1111/j.1461-0248.2011.01605.x

Nuismer, S. L. (2006). Parasite local adaptation in a geographic mosaic. *Evolution*, *60*(1), 24–30. https://doi.org/10.1111/j.0014-3820.2006.tb01078.x

Nuismer, S. L., & Kirkpatrick, M. (2003). Gene flow and the coevolution of parasite range. *Evolution*, *57*(4), 746–754. https://doi.org/10.1111/j.0014-3820.2003.tb00286.x

O'Brien, M. J., Carbonell, E. P., Losapio, G., Schlüter, P. M., & Schöb, C. (2020). Foundation species promote local adaptation and fine-scale distribution of herbaceous plants. *Journal of Ecology*, *109*(1), 191–203. https://doi.org/10.1111/1365-2745.13461

Orr, H. A., & Unckless, R. L. (2008). Population extinction and the genetics of adaptation. *The American Naturalist*, *172*(2), 160–169. https://doi.org/10.1086/589460

Otto, S. P., & Day, T. (2007). Evolutionary invasion analysis. In *A biologist's guide to mathematical modeling in ecology and evolution* (pp. 454–512). Princeton University Press.

Paaby, A. B., & Rockman, M. V. (2014). Cryptic genetic variation: Evolution's hidden substrate. *Nature Reviews Genetics*, *15*(4), 247–258. https://doi.org/10.1038/nrg3688

Pannell, J. R. (2016, August). Evolution of the mating system in colonizing plants. In *Invasion genetics* (pp. 57–80). https://doi.org/10.1002/9781119072799.ch4

Pease, C. M., Lande, R., & Bull, J. J. (1989). A model of population growth, dispersal and evolution in a changing environment. *Ecology*, *70*(6), 1657–1664. https://doi.org/10.2307/1938100

Polechová, J. (2018). Is the sky the limit? On the expansion threshold of a species' range. *PLOS Biology*, *16*(6), e2005372. https://doi.org/10.1371/journal.pbio.2005372

Polechová, J., & Barton, N. H. (2015). Limits to adaptation along environmental gradients. *Proceedings of the National Academy of Sciences*, *112*(20), 6401–6406. https://doi.org/10.1073/pnas.1421515112

Prieto, I., Kikvidze, Z., & Pugnaire, F. I. (2010). Hydraulic lift: Soil processes and transpiration in the Mediterranean leguminous shrub *Retama sphaerocarpa* (L.) Boiss. *Plant and Soil*, *329*(1), 447–456. https://doi.org/10.1007/s11104-009-0170-3

Proulx, S. R. (2002). Niche shifts and expansion due to sexual selection. *Evolutionary Ecology Research*, *4*(3), 351–369.

Pugnaire, F. I., Armas, C., & Maestre, F. T. (2011). Positive plant interactions in the Iberian Southeast: Mechanisms, environmental gradients, and ecosystem function. *Journal of Arid Environments*, *75*(12), 1310–1320. https://doi.org/10.1016/j.jaridenv.2011.01.016

R Core Team. (2025). R: A language and environment for statistical computing.

Raath-Krüger, M. J., Schöb, C., McGeoch, M. A., & le Roux, P. C. (2021). Interspecific facilitation mediates the outcome of intraspecific interactions across an elevational gradient. *Ecology*, *102*(1), e03200. https://doi.org/10.1002/ecy.3200

Richardson, J. L., Urban, M. C., Bolnick, D. I., & Skelly, D. K. (2014). Microgeographic adaptation and the spatial scale of evolution. *Trends in Ecology & Evolution*, *29*(3), 165–176. https://doi.org/10.1016/j.tree.2014.01.002

Ronce, O. (2007). How does it feel to be like a rolling stone? Ten questions about dispersal evolution. *Annual Review of Ecology, Evolution, and Systematics*, *38*, 231–253. https://doi.org/10.1146/annurev.ecolsys.38.091206.095611

Ronce, O., & Kirkpatrick, M. (2001). When sources become sinks: Migrational meltdown in heterogeneous habitats. *Evolution*, *55*(8), 1520–1531. https://doi.org/10.1111/j.0014-3820.2001.tb00672.x

Sasaki, A., & de Jong, G. (1999). Density dependence and unpredictable selection in a heterogeneous environment: Compromise and polymorphism in the ESS reaction norm. *Evolution*, *53*(5), 1329–1342. https://doi.org/10.1111/j.1558-5646.1999.tb05398.x

Schiffers, K., Schurr, F. M., Travis, J. M. J., Duputié, A., Eckhart, V. M., Lavergne, S., McInerny, G., Moore, K. A., Pearman, P. B., Thuiller, W., Wüest, R. O., & Holt, R. D. (2014). Landscape structure and genetic architecture jointly impact rates of niche evolution. *Ecography*, *37*(12), 1218–1229. https://doi.org/10.1111/ecog.00768

Soliveres, S., Eldridge, D. J., Maestre, F. T., Bowker, M. A., Tighe, M., & Escudero, A. (2011). Microhabitat amelioration and reduced competition among understorey plants as drivers of facilitation across environmental gradients: Towards a unifying framework. *Perspectives in Plant Ecology, Evolution and Systematics*, *13*(4), 247–258. https://doi.org/10.1016/j.ppees.2011.06.001

Suggitt, A. J., Wilson, R. J., Isaac, N. J. B., Beale, C. M., Auffret, A. G., August, T., Bennie, J. J., Crick, H. Q. P., Duffield, S., Fox, R., Hopkins, J. J., Macgregor, N. A., Morecroft, M. D., Walker, K. J., & Maclean, I. M. D. (2018). Extinction risk from climate change is reduced by microclimatic buffering. *Nature Climate Change*, *8*(8), 713–717. https://doi.org/10.1038/s41558-018-0231-9

Tirado, R., & Pugnaire, F. I. (2003). Shrub spatial aggregation and consequences for reproductive success. *Oecologia*, *136*(2), 296–301. https://doi.org/10.1007/s00442-003-1264-x

Tufto, J. (2001). Effects of releasing maladapted individuals: A demographic-evolutionary model. *The American Naturalist*, *158*(4), 331–340. https://doi.org/10.1086/321987

Uecker, H., & Hermisson, J. (2016). The role of recombination in evolutionary rescue. *Genetics*, *202*(2), 721–732. https://doi.org/10.1534/genetics.115.180299

Urban, M. C., Scarpa, A., Travis, J. M. J., & Bocedi, G. (2019). Maladapted prey subsidize predators and facilitate range expansion. *The American Naturalist*, *194*(4), 590–612. https://doi.org/10.1086/704780

Valiente-Banuet, A., Rumebe, A. V., Verdú, M., & Callaway, R. M. (2006). Modern quaternary plant lineages promote diversity through facilitation of ancient tertiary lineages. *Proceedings of the National Academy of Sciences*, *103*(45), 16812–16817. https://doi.org/10.1073/pnas.0604933103

Valiente-Banuet, A., & Verdú, M. (2007). Facilitation can increase the phylogenetic diversity of plant communities. *Ecology Letters*, *10*(11), 1029–1036. https://doi.org/10.1111/j.1461-0248.2007.01100.x

van der Heijden, M. G. A., & Horton, T. R. (2009). Socialism in soil? The importance of mycorrhizal fungal networks for facilitation in natural ecosystems. *Journal of Ecology*, *97*(6), 1139–1150. https://doi.org/10.1111/j.1365-2745.2009.01570.x

Verdú, M., Gómez, J. M., Valiente-Banuet, A., & Schöb, C. (2021). Facilitation and plant phenotypic evolution. *Trends in Plant Science*, *26*(9), 913–923. https://doi.org/10.1016/j.tplants.2021.04.005

Vicente-Serrano, S. M., Lopez-Moreno, J.-I., Beguería, S., Lorenzo-Lacruz, J., Sanchez-Lorenzo, A., García-Ruiz, J. M., Azorin-Molina, C., Morán-Tejeda, E., Revuelto, J., Trigo, R., Coelho, F., & Espejo, F. (2014). Evidence of increasing drought severity caused by temperature rise in southern Europe. *Environmental Research Letters*, *9*(4), 044001. https://doi.org/10.1088/1748-9326/9/4/044001

Vogel, J. P., Tuna, M., Budak, H., Huo, N., Gu, Y. Q., & Steinwand, M. A. (2009). Development of SSR markers and analysis of diversity in Turkish populations of *Brachypodium distachyon*. *BMC Plant Biology*, *9*(1), 88. https://doi.org/10.1186/1471-2229-9-88

Willi, Y., & Hoffmann, A. A. (2009). Demographic factors and genetic variation influence population persistence under environmental change. *Journal of Evolutionary Biology*, *22*(1), 124–133. https://doi.org/10.1111/j.1420-9101.2008.01631.x

Wright, I. J., Reich, P. B., Cornelissen, J. H. C., Falster, D. S., Garnier, E., Hikosaka, K., Lamont, B. B., Lee, W., Oleksyn, J., Osada, N., Poorter, H., Villar, R., Warton, D. I., & Westoby, M. (2005). Assessing the generality of global leaf trait relationships. *New Phytologist*, *166*(2), 485–496. https://doi.org/10.1111/j.1469-8137.2005.01349.x